Sensitivity of stratospheric geoengineering with black carbon to aerosol size and altitude of injection

Ben Kravitz,[1] Alan Robock,[2] Drew T. Shindell,[3] and Mark A. Miller[2]

Received 16 December 2011; revised 20 February 2012; accepted 19 March 2012; published 4 May 2012.

[1] Simulations of stratospheric geoengineering with black carbon (BC) aerosols using a general circulation model with fixed sea surface temperatures show that the climate effects strongly depend on aerosol size and altitude of injection. 1 Tg BC a^{-1} injected into the lower stratosphere would cause little surface cooling for large radii but a large amount of surface cooling for small radii and stratospheric warming of over 60°C. With the exception of small particles, increasing the altitude of injection increases surface cooling and stratospheric warming. Stratospheric warming causes global ozone loss by up to 50% in the small radius case. The Antarctic shows less ozone loss due to reduction of polar stratospheric clouds, but strong circumpolar winds would enhance the Arctic ozone hole. Using diesel fuel to produce the aerosols is likely prohibitively expensive and infeasible. Although studying an absorbing aerosol is a useful counterpart to previous studies involving sulfate aerosols, black carbon geoengineering likely carries too many risks to make it a viable option for deployment.

Citation: Kravitz, B., A. Robock, D. T. Shindell, and M. A. Miller (2012), Sensitivity of stratospheric geoengineering with black carbon to aerosol size and altitude of injection, *J. Geophys. Res.*, *117*, D09203, doi:10.1029/2011JD017341.

1. Introduction

[2] Geoengineering with stratospheric sulfate aerosols has, in recent years, become a commonly discussed means of alleviating some of the potential negative consequences of anthropogenic climate change by backscattering a portion of sunlight to space [*Crutzen*, 2006]. Climate modeling research into this topic has a long history [*Govindasamy and Caldeira*, 2000; *Rasch et al.*, 2008; *Robock et al.*, 2008], and is ongoing, in particular in the form of the Geoengineering Model Intercomparison Project (GeoMIP), which provides a standardized suite of four experiments to be conducted by the different climate modeling groups in an attempt to ascertain the robust features of the climate impacts of stratospheric sulfate aerosol geoengineering [*Kravitz et al.*, 2011].

[3] Despite these large research efforts, comparatively little attention has been paid to other choices of aerosol, probably because sulfate aerosols have the well understood natural analogue of large volcanic eruptions. Engineered particles, such as resonant scatterers or self-levitating particles, have been proposed, but the feasibility of using these aerosols has yet to be determined [*Teller et al.*, 1997; *Keith*, 2010]. One possibility which has been suggested repeatedly but received little formal attention is black carbon aerosols [*Teller et al.*, 1997, 2002; *Lane et al.*, 2007; *Crutzen*, 2006]. This idea has analogues in the form of large fires [*Robock*, 1988, 1991; *Fromm et al.*, 2010] and simulations of nuclear winter [*Turco et al.*, 1983; *Robock et al.*, 2007a, 2007b; *Toon et al.*, 2007; *Mills et al.*, 2008].

[4] The climate effects of black carbon aerosol geoengineering have the potential to be severe, mostly due to stratospheric heating [*Ferraro et al.*, 2011]. In particular, as in nuclear winter simulations, one potential consequence is catastrophic ozone loss [*Toon et al.*, 2007; *Mills et al.*, 2008]. However, one advantage black carbon could have over sulfate aerosols is that less aerosol mass is needed, which could mediate the expected negative impacts. For example, more radiatively efficient particles means less aerosol mass would be required to achieve a desired level of surface cooling. Also, aerosols that stay in the atmosphere longer require a lower replenishment rate.

[5] These factors can largely be controlled by particle size and altitude of injection. Smaller particles have slower fall speeds and are more radiatively efficient, meaning less is needed, and the degree of solar absorption and consequent self-lofting is greater. Particles injected at higher altitudes have a longer distance to fall and are less susceptible to stratospheric removal processes, like midlatitude tropopause folds, and scavenging by deep convective clouds, although if the particles are self-lofting, as is the case for black carbon aerosols, this becomes less of an issue [*Rohatschek*, 1996; *Pueschel et al.*, 2000]. *Ban-Weiss et al.* [2012] already

[1]Department of Global Ecology, Carnegie Institution for Science, Stanford, California, USA.
[2]Department of Environmental Sciences, Rutgers University, New Brunswick, New Jersey, USA.
[3]NASA Goddard Institute for Space Studies, New York, New York, USA.

Corresponding Author: B. Kravitz, Department of Global Ecology, Carnegie Institution for Science, 260 Panama St., Stanford, CA 94305, USA. (bkravitz@carnegie.stanford.edu)

0148-0227/12/2011JD017341

Table 1. The Different Experiments and Parameter Choices Used in This Study[a]

Ensemble Name	Description	Particle Radius (μm)	Altitude of Injection (mb)
Con	Control run (constant 2000 conditions)		
Def	Default	0.08	100–150
HA	High Altitude	0.08	20–57
SmR	Small Radius	0.03	100–150
LgR	Large Radius	0.15	100–150
HALgR	High Altitude + Large Radius	0.15	20–57

[a]All geoengineering experiments involved injection of 1 Tg a^{-1} of black carbon aerosols throughout the altitudes listed in column 4.

performed some work on sensitivity to altitude of injection, but they used prescribed aerosol layers, meaning their investigation did not analyze circulation patterns in as much detail as our study, nor could they explore the role of self-lofting.

[6] Thus we have several motivations for our study. The first is to determine some of the expected radiative and climatic perturbations of stratospheric geoengineering with black carbon aerosols. The second is to determine the sensitivity of black carbon aerosol geoengineering to aerosol size and altitude of injection, including changes in circulation. A third task is an assessment of means by which this method of geoengineering might be done, the projected costs of doing so, and the emissions factors that might result.

[7] Our investigations are primarily radiative in nature. Although interactive chemistry is an important part of our simulations, specifically regarding the effects on ozone, our discussion of chemical effects is purposefully limited. A more detailed investigation of these effects with a coupled chemistry model would certainly be warranted. Moreover, certain aspects of chemical effects pertaining to black carbon aerosols, notably heterogeneous chemistry on the aerosol surfaces, are a large source of uncertainty, and as such, are poorly represented in the model [*Nienow and Roberts*, 2006]. The climate model we use (Section 2) is an excellent tool for investigating the questions contained in this paper, but more intricate processes require tools which are beyond the capacity of our study.

2. Experiment Design

[8] We conducted our simulations with GISS ModelE2, a general circulation model developed by NASA's Goddard Institute for Space Studies (previous version: *Schmidt et al.* [2006]). The version of the model we used has horizontal resolution of 2° latitude by 2.5° longitude and 40 vertical layers extending up to 0.1 mb (~80 km). We ran the model using full stratospheric chemistry, where ozone is both radiatively and chemically interactive with the climate. The model is able to reproduce realistic ozone values and chemical ozone depletion, and stratospheric ozone at middle and high latitudes is considerably more realistic in the new ModelE2 than that shown in *Shindell et al.* [2006]. Our background case was constant year 2000 conditions in the atmosphere, and both sea surface temperatures (SSTs) and sea ice were fixed at an average of year 1996–2005, prescribed by HadISST [*Rayner et al.*, 2003]. Although using fixed SSTs will affect temperature and circulation patterns, it is a useful means of isolating stratospheric responses and is a standard method in the CCMVal simulations [*SPARC CCMVal*, 2010]. Each experiment ensemble has three members of ten-year simulations. The control ensemble was conducted with constant year 2000 conditions in which greenhouse gases, background aerosols, and other radiatively important features were held fixed.

[9] Treatment of black carbon aerosols in this model, specifically surface adsorption of organic compounds, is discussed in detail by *Hansen et al.* [2007]. Briefly, absorption calculated for external mixing is increased by a factor of two to account for internal mixing [*Chylek et al.*, 1995], and black carbon and organic carbon particles are scaled so they match AERONET observations [*Koch*, 2001; *Sato et al.*, 2003]. This factor of two was derived for tropospheric emissions, so we are uncertain of how reasonable an assumption this is for stratospheric conditions. Although our aerosol model has a fixed, prescribed size distribution and no microphysics, meaning a more sophisticated model is necessary to test this assumption, such a test would certainly be warranted in the future.

[10] All geoengineering experiments involved continuous injections of BC aerosols into three adjacent vertical model layers in the stratosphere, totaling 1 Tg per year. The aerosols were placed along the 0° longitude meridian between 10°S and 10°N. The injection altitude and initial particle radius were varied to determine the sensitivity of the climate effects to these parameters. To assess sensitivity of geoengineering to particle radius, we chose three aerosol dry radii: 0.03 μm, 0.08 μm, and 0.15 μm, which are particle sizes typical of black carbon aerosols [*Rose et al.*, 2006]. The model hydrates these aerosols, and they hygroscopically grow according to formulas by *Tang* [1996]. However, at these sizes, growth is no more than 0.02–0.03 μm. We also tested two altitudes of injection: lower stratosphere (100–150 mb) and middle stratosphere (20–57 mb). The different experiments are summarized in Table 1.

[11] One experiment not listed in Table 1 is the combination of high altitude and small radius. The model failed to simulate this scenario, as 1 Tg a^{-1} of black carbon aerosol injection caused excessive ozone loss and stratospheric heating. To ensure comparability of our experiments, we chose not to simulate this scenario with a smaller injection rate.

3. Black Carbon Mass Loading and Deposition

[12] Atmospheric lifetime will affect the peak mass loading of the aerosols. Figure 1 shows globally averaged stratospheric BC aerosol mass for each of the five ensembles in Table 1. The large aerosol size in the LgR simulation results in a high fall rate, so only this ensemble has reached steady state by the end of the ten-year simulation. The highest mass loading in the figure is for ensemble HA, reaching a globally

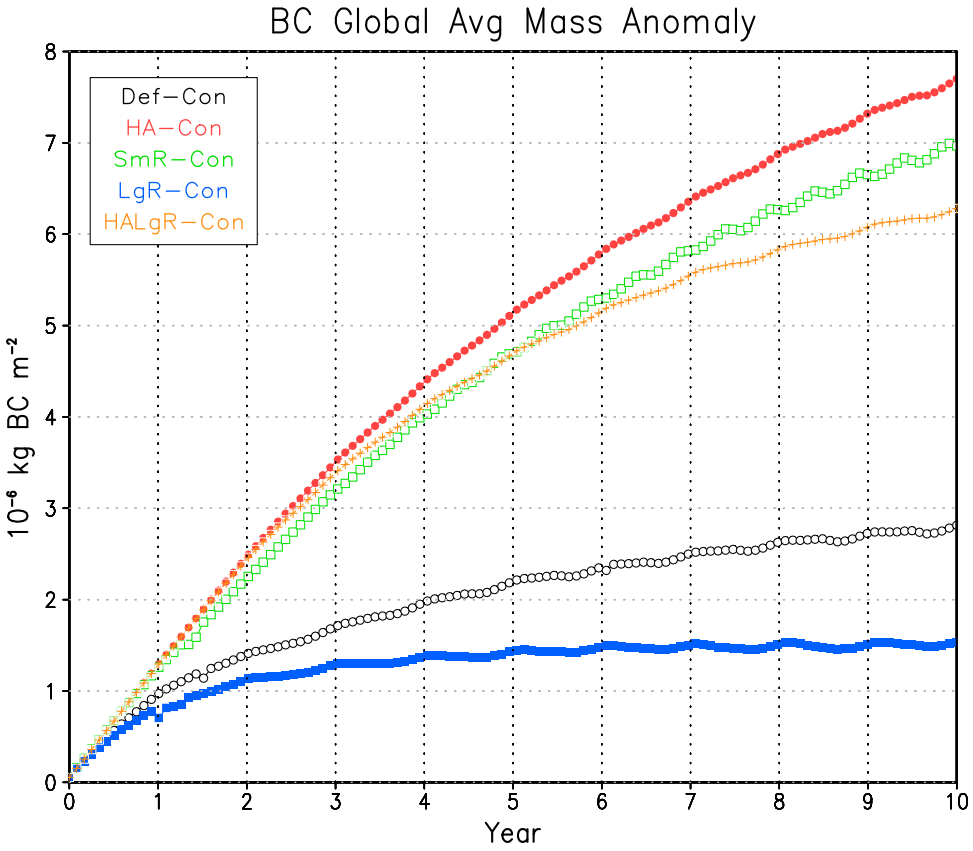

Figure 1. Globally averaged black carbon mass anomaly (experiment minus control) for each of the five ensembles in Table 1.

averaged mass loading of 7.7×10^{-6} kg BC m^{-2} by year ten, or approximately 90% of its steady state value, based on a simple mass balance equation (Table 2).

[13] With the exception of ensemble SmR, the mass loadings of the simulations can be divided into two groups which depend on the altitude of injection, where aerosols injected at higher altitudes have a longer lifetime. According to the values in Table 2, the equilibrium mass burden in Tg BC and the *e*-folding lifetime in years (the same number, since the injection rate is 1 Tg BC a^{-1}) for the two groups are separated by more than a factor of two. Our simulations show that unless the particles are small, altitude is the dominant factor in determining the steady state mass loading. LgR shows the lowest *e*-folding lifetime of all of the experiments, at 0.75 years, which is even lower than the 1 year *e*-folding lifetime for sulfate aerosols, both in terms of large tropical volcanic eruptions and tropical geoengineering with stratospheric SO_2 injections [*Stenchikov et al.*, 1998; *Robock et al.*, 2008].

[14] Figure 2 shows spatially resolved black carbon mass burden in the stratosphere. The bulk of the aerosols stay near the altitude of injection, although self-lofting of the aerosols is readily apparent, with the model showing aerosol mass extending to the model top (80 km), which was also found by *Mills et al.* [2008] in their nuclear winter simulations. Although the steady state atmosphere loading amounts for SmR and HA are similar (3.77 and 4.26 Tg BC, respectively), the peak values in Figure 2 for HA are twice those of SmR. The range of altitudes covered by the two ensembles is similar, implying the aerosols in SmR are more evenly distributed vertically than in HA. In the Def experiment, particles generally do not reach the mesosphere. The only difference between this experiment and experiment HA is the altitude of injection, implying the rate of stratospheric removal is higher for experiment Def. Experiment LgR shows little excursion of the aerosols from the altitudes into which they are injected, and the amount of aerosols in the stratosphere is lower than for all other experiments.

[15] Eventually, the aerosols will pass into the troposphere, generally through midlatitude tropopause folds or large scale circulation during the polar winter. Figure 3 shows total deposition rates for each of the ensembles. The model accounts for precipitation scavenging of particles and gravitational settling, but in our simulations, wet deposition

Table 2. Atmospheric Loading and *e*-Folding Lifetimes of Black Carbon Aerosols for Each Geoengineering Scenario[a]

Ensemble	Equilibrium Mass Burden (Tg BC) and *e*-Folding Lifetime (years)
Def	1.40
HA	4.26
SmR	3.77
LgR	0.75
HALgR	3.31

[a]Values in column 2 are calculated from Figure 1 by a simple mass balance equation $m(t) = \frac{S}{k}(1 - e^{-kt})$, where m is mass, S is the source term, t is time, and k is a constant. Equilibrium is reached when $t \rightarrow \infty$, or $m = \frac{S}{k}$. Because atmospheric loading is 1 Tg BC a^{-1}, values in the second column are both equilibrium mass and *e*-folding lifetime.

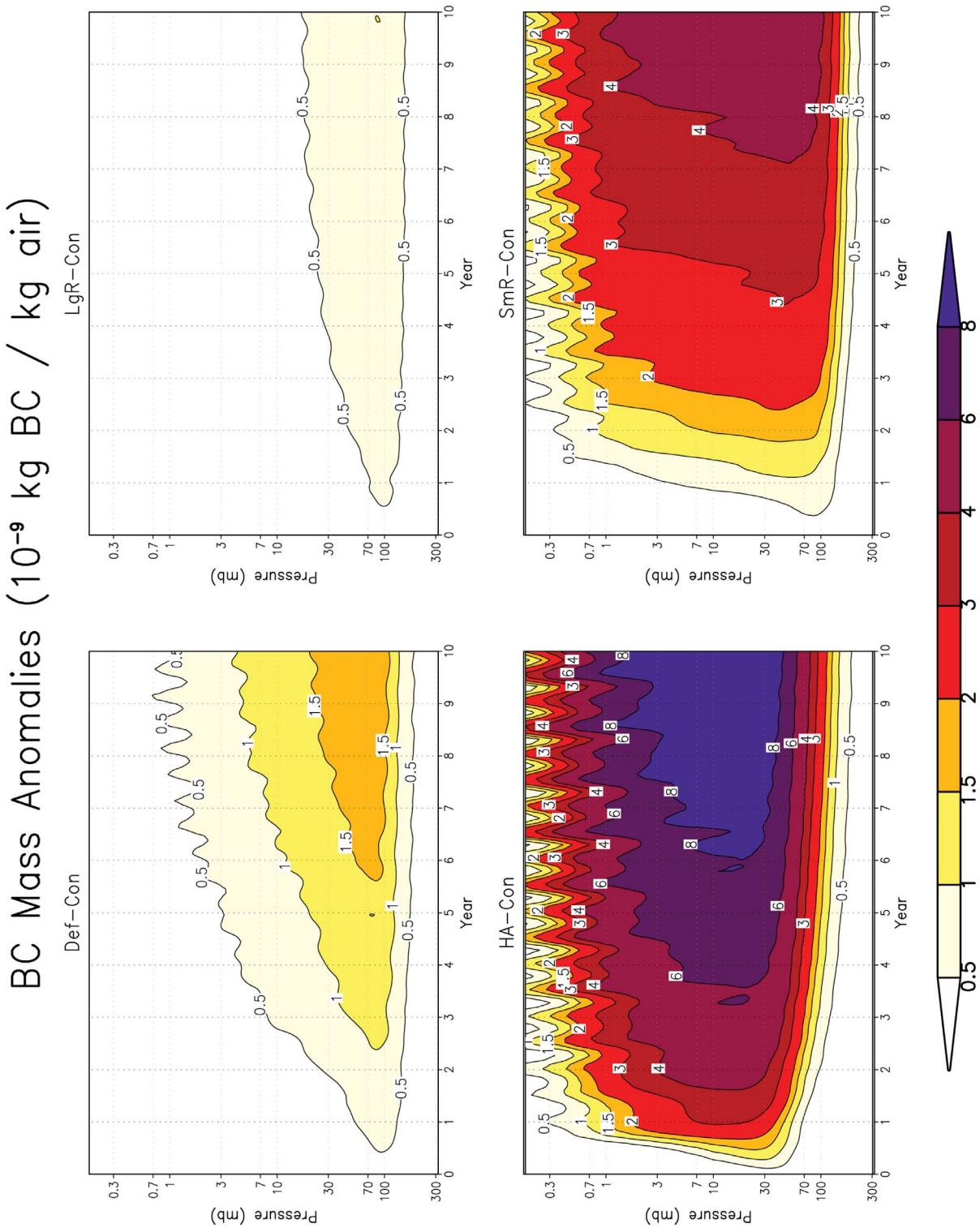

Figure 2. Vertically resolved global average black carbon mass anomalies for changing radius and altitude. Only upper tropospheric and stratospheric altitudes (pressure < 300 mb) are shown. Ensemble descriptions are given in Table 1.

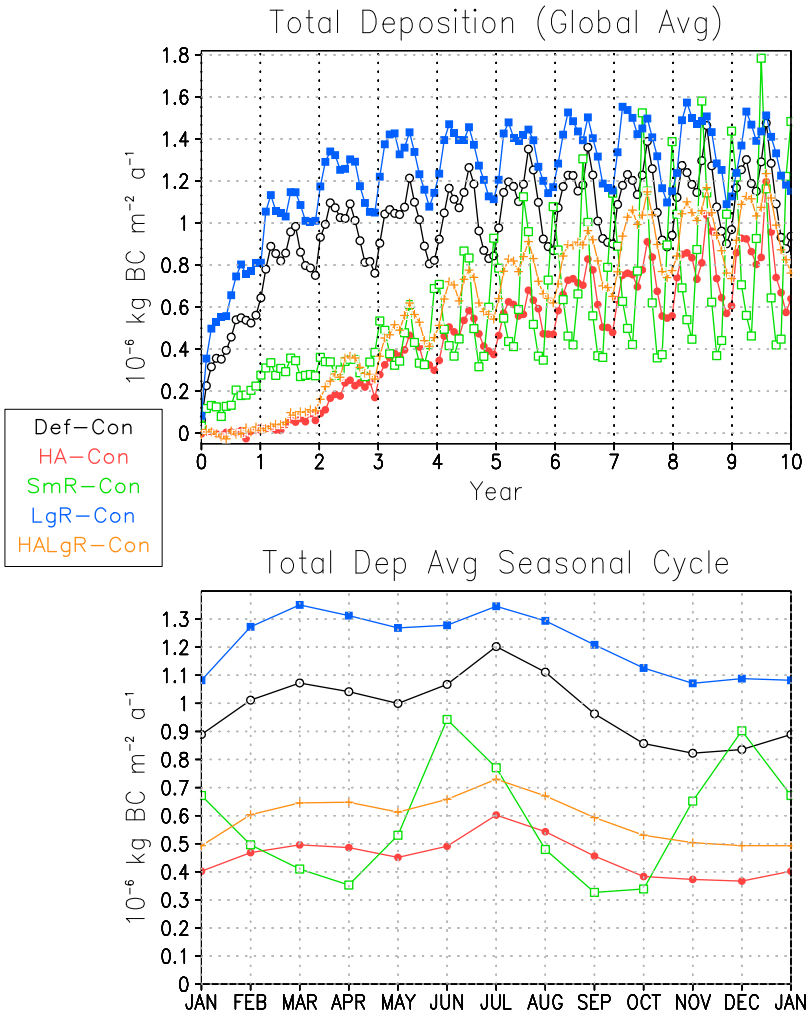

Figure 3. Globally averaged total (wet + dry) deposition of black carbon for each of the five ensembles in Table 1. (top) Just the global average, and (bottom) the average seasonal cycle, calculated over the last three years of simulation (years 8–10).

accounted for over 90% of the total. This is in contrast to simulations of stratospheric sulfate aerosol geoengineering with an earlier version of the same model, which resulted in approximately 67% of total deposition being due to precipitation scavenging [*Kravitz et al.*, 2009].

[16] Deposition rates come close to steady state for all ensembles by the end of the ten-year simulations (Figure 3). Again, with the exception of SmR, the curves in Figure 3 can be divided into two different categories, with the high altitude injections having a lower deposition rate than the low altitude injections. Aerosols injected at low altitudes are more susceptible to being caught in tropopause folds and being scavenged by tropical deep convective clouds extending into the lower stratosphere. With the exception of ensemble SmR, all experiments show a noticeable seasonal cycle with a peak in boreal spring and summer, with Def and LgR showing a stronger seasonal cycle than HA and HALgR. SmR shows distinct peaks in the summer of each hemisphere.

[17] To determine the reasons for these peaks, we examine spatial maps of deposition (Figure 4). In Def and LgR, large swaths of the midlatitudes show an increase in deposition. Aerosols in these two experiments remain concentrated in the lower stratosphere, where tropopause fold occurrence reaches a maximum during spring and summer [*Van Haver et al.*, 1996]. The maximum is less pronounced for tropopause folding events involving higher stratospheric altitudes, but still present, explaining the midlatitude anomalies in ensemble HA. In these three experiments, Northern Hemisphere anomalies are larger than Southern Hemisphere anomalies, simply because the atmospheric mass burden of black carbon aerosols tends to favor the Northern Hemisphere (not pictured).

[18] Ensemble SmR does not have these anomalies in the midlatitudes, possibly implying tropopause folding is not a dominant mechanism of stratospheric removal for these aerosols. At this time, we are unable to ascertain a reason for this phenomenon and suggest a more thorough analysis of stratospheric dynamics in this experiment be conducted in the future.

[19] Polar deposition increases compared to the control ensemble in all four geoengineering ensembles, but most dramatically in ensemble SmR. This occurs during the polar summer, which explains the double peak for ensemble SmR in Figure 3. The other three ensembles show smaller

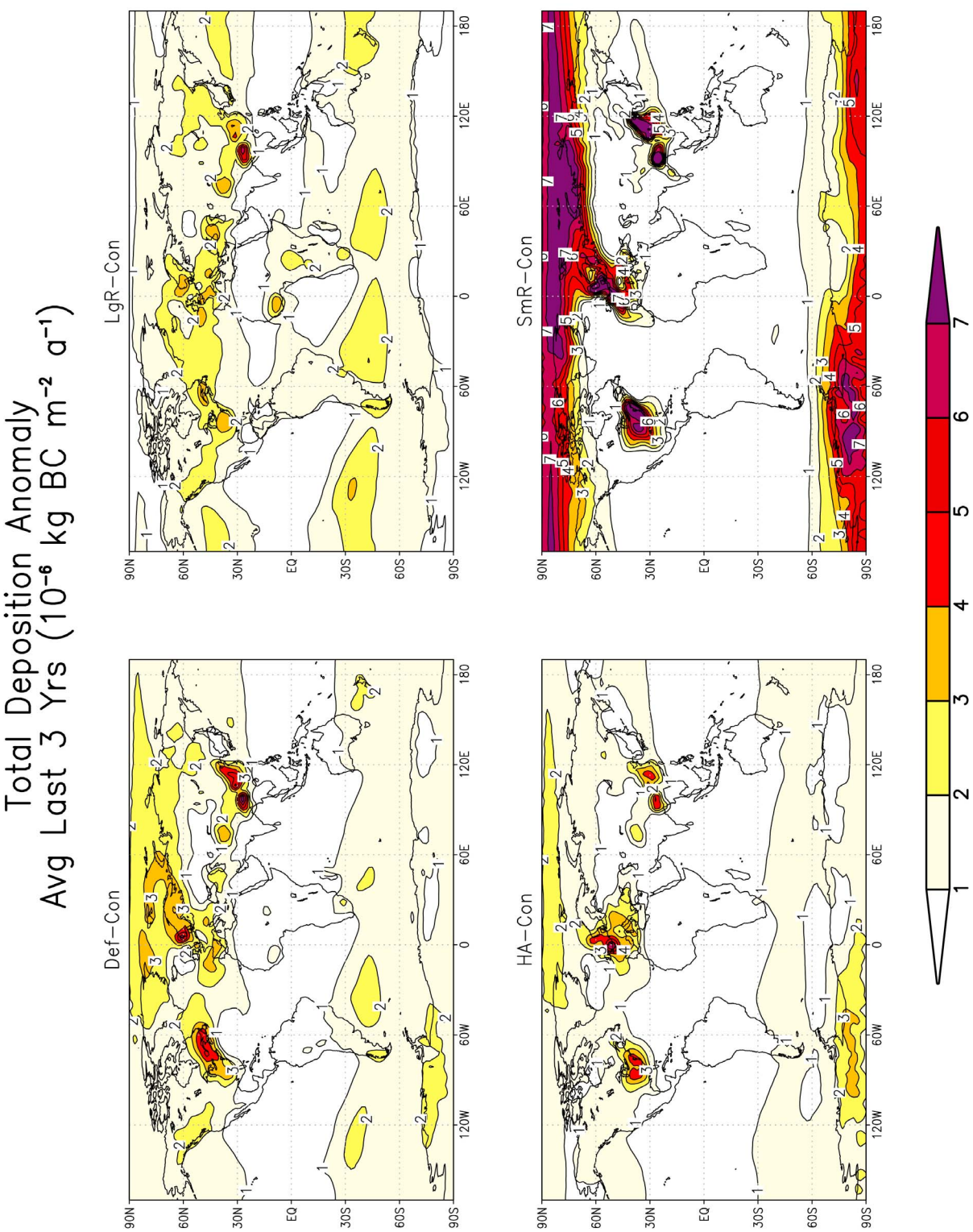

Figure 4. Anomalies in total (wet + dry) deposition for four of the geoengineering ensembles, averaged over the last three years of simulation (years 8–10). Ensemble descriptions are given in Table 1.

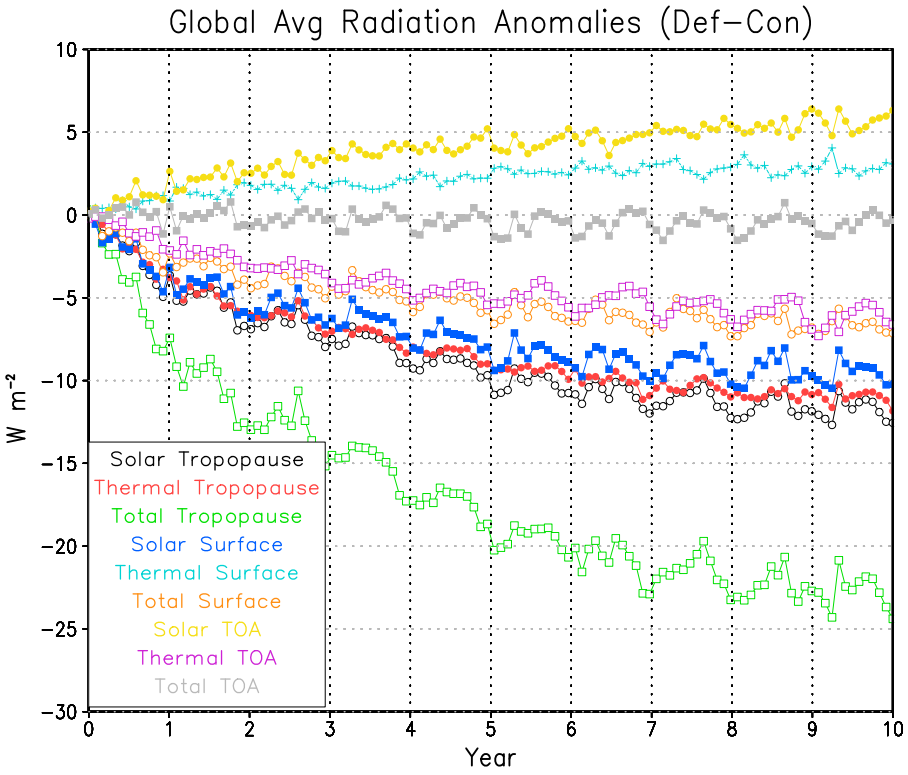

Figure 5. Globally averaged radiation anomalies (solar, thermal, and total) at the top of atmosphere (TOA), tropopause, and surface for ensemble Def. Positive values indicate more downward than upward flux. Calculations corresponding to this figure, as well as for other ensembles, are in Table 3.

increases in polar deposition. (Although polar deposition reaches similar values, the area over the poles is much smaller than the area over the midlatitudes, so globally averaged deposition is dominated by tropopause folding in these experiments.)

[20] One possible mechanism is that aerosols become trapped in the strengthened polar vortices (discussed in Section 6) and circulate around the poles until the summers, during which temperatures are warm enough for precipitation events. However, a great deal of further investigation is required to ascertain the viability of this mechanism.

[21] An additional phenomenon in Figure 4 is the increase in black carbon deposition over areas which appear to be urban centers or large sources of anthropogenic aerosols. These anomalies potentially imply a fundamental change in deposition mechanisms due to black carbon geoengineering. The apparent alignment may also be a coincidence, as these areas also have high summer rainfall. Further investigation is needed, but we are currently unable to ascertain a reason for this effect.

4. Radiative Perturbations

[22] The primary purpose of geoengineering is to perturb the radiative budget of the planet. Figure 5 shows anomalies in globally averaged radiation quantities (solar, thermal, and total), calculated at the top of atmosphere (TOA), tropopause, and surface for the Def ensemble. Other ensembles show similar separation of the nine different curves, albeit with different values (not pictured).

[23] Positive (where net is measured as down minus up) solar TOA radiation means less solar radiation is leaving the planet in the Def experiment than in the control ensemble, which is consistent with a stratospheric layer of absorbing aerosols. Thermal TOA radiation is also consistent with this layer, as a heated stratosphere will radiate more thermal energy to space. Negative total TOA radiation shows that more energy is being radiated to space in the Def experiment than in the control experiment, which implies cooling of the surface and atmosphere by the Stefan-Boltzmann law.

[24] At the tropopause, just below the aerosol layer in the Def experiment, all three radiation quantities are negative. Solar is negative because of the reduced amount of solar radiation reaching the tropopause. Because tropopause temperatures are raised significantly (discussed in Section 6), the warmer tropopause region loses more thermal radiation to space, but the relative temperature difference between the tropopause and the mesosphere or thermosphere, where radiative impacts are small, is larger than the relative difference between the tropopause and the surface, meaning net thermal radiation at the tropopause should be dominated by upward thermal radiation to space, i.e., tropopause thermal radiation should have negative values.

[25] The atmosphere is relatively transparent to solar radiation, so solar radiation at the tropopause and surface are, expectedly, similar. Thermal radiation at the surface is

Table 3. Mass-Normalized Radiative Efficiency for Black Carbon Aerosols for Each Experiment[a]

	Def	HA	SmR	LgR	HALgR
Solar (TOA)	1.99	2.15	6.27	0.62	0.99
Thermal (TOA)	−2.19	−3.10	−8.24	−0.71	−1.49
Total (TOA)	−0.20	−0.95	−1.97	−0.09	−0.50
Solar (Tropopause)	−4.39	−3.34	−10.42	−2.34	−1.83
Thermal (Tropopause)	−4.09	−2.34	−8.31	−2.28	−1.32
Total (Tropopause)	−8.48	−5.68	−18.73	−4.62	−3.15
Solar (Surface)	−3.60	−2.75	−8.39	−2.03	−1.46
Thermal (Surface)	1.11	0.51	1.78	0.71	0.30
Total (Surface)	−2.49	−2.23	−6.61	−1.32	−1.16

[a]Radiation quantities investigated are net solar, thermal, and total (solar + thermal) radiation anomalies (geoengineering minus control) at the top of atmosphere (TOA), tropopause, and surface. Each quantity is normalized by the total black carbon mass loading and then averaged over the last five years of simulation. Net values given are calculated as down minus up. Units are in megawatts per kilogram of black carbon. All values are rounded to two decimal places.

positive, which is consistent with surface cooling and subsequent reduced upward radiation.

[26] To compare the radiative efficiencies of the anomalies in each ensemble, we normalize radiation by the atmospheric mass loading to get units of W (kg BC)$^{-1}$, as in Table 3. As expected, smaller particles are more efficient at perturbing all radiation fields, with values in the SmR column dominating the table. All higher altitude injection experiments, when compared to their corresponding lower altitude experiments, show a reduced (in magnitude) radiative efficiency for the tropopause and surface, and a greater efficiency at TOA. However, this apparent dependence on altitude is artificial, in that for the higher altitude injection experiments, more aerosols are higher in altitude and farther from the tropopause, so the amount of radiative perturbation to TOA is more than for lower altitudes, and the perturbations to the tropopause and surface are less.

5. Surface Temperature Effects

[27] As the radiative perturbations show, geoengineering with black carbon aerosols does cool the surface, albeit by highly variable amounts depending upon the ensemble. However, showing results for globally averaged surface air temperature anomalies would not be particularly useful, as our simulations were conducted with fixed sea surface temperatures, which precludes the ability of the ocean to respond to radiative forcing. However, *Hansen et al.* [2007] showed that for fixed sea surface temperatures, one can obtain a reliable estimate of the expected surface temperature response by multiplying the TOA total radiation perturbation by the model's climate sensitivity, as we have done in Table 4.

[28] According to the results of Table 4, under the specifications of ensemble Def, 1 Tg of black carbon aerosols injected into the stratosphere each year could cool the climate to levels observed approximately 25–30 years ago [*Hansen et al.*, 2010]. Assuming temperature response scales linearly with injection amount, achieving the same amount of cooling under the specifications of ensembles HA, SmR, LgR, and HALgR would require annual injections of 0.08, 0.04, 6.70, and 0.18 Tg, respectively.

[29] Ensemble Def shows surface air temperature cooling by 0.38°C, or a return to approximately 1980 temperature levels. This ensemble shows the most reasonable value of cooling, as LgR shows barely distinguishable cooling, and the others show over 2°C of cooling, to well below preindustrial levels. A temperature anomaly of −0.38°C is similar to the values simulated by *Robock et al.* [2008] in their experiment of tropical injections of 5 Tg a^{-1} SO_2. Therefore, in our discussions of stratospheric heating and its consequences in the following section, we concentrate on this scenario.

6. Consequences of Stratospheric Heating

[30] Placing a large amount of absorbing aerosols in the stratosphere will cause stratospheric heating. Figure 6 shows globally averaged, vertically resolved stratospheric temperature anomalies for four ensembles. Ensemble LgR shows modest stratospheric heating concentrated near the tropopause. Ensemble SmR shows the largest heating, in some grid boxes by 80°C. Def and SmR show cooling anomalies in the mesosphere, whereas ensemble HA shows heating throughout the entire upper atmosphere. Values in ensemble HA are similar to those found by *Mills et al.* [2008] in their nuclear winter simulations.

[31] Figure 7 shows the vertical temperature profiles for all ensembles. LgR shows only a slight departure from the control ensemble, with all other ensembles showing greater stratospheric warming. In most of the ensembles, the tropopause is pushed downward by the stratospheric heating. The tropopause is the point at which the combined heat radiation from the surface (from absorption of solar radiation) and heat radiation from the stratospheric ozone layer (from absorption of ultraviolet radiation) is at a minimum. Stratospheric heating changes this height, resulting in a lower tropopause. Similarly, the stratopause is the height of a local maximum in temperature due to heating from UV absorption. The ozone loss from black carbon geoengineering (discussed below) lowers the stratopause and causes mesospheric cooling, explaining the negative temperature anomalies in Figure 6. In the SmR experiment, heating is strong enough to destabilize the stratosphere. Further study is needed to determine the dynamical implications of this.

[32] One of the consequences of stratospheric heating is ozone loss. *Mills et al.* [2008] discuss the stratospheric

Table 4. Estimates of Globally Averaged Surface Air Temperature Changes for Each Experiment of Black Carbon Aerosol Geoengineering[a]

	Def	HA	SmR	LgR	HALgR
ΔR (W m^{-2})	−0.55	−7.03	−13.50	−0.08	−3.04
σ (W m^{-2})	0.52	0.62	1.02	0.37	0.64
ΔT estimate (°C)	−0.38	−4.92	−9.45	−0.06	−2.13

[a]The first row, denoted by ΔR, is the globally averaged total (solar + thermal) radiation anomaly (geoengineering minus control) at TOA, averaged over the last year of simulation. The second row (σ) is the standard deviations of the radiation anomalies for the last year. The values in the first row are multiplied by 0.7°C W^{-1} m^2, the climate sensitivity of this version of ModelE2 (G. Schmidt, personal communication, 2011) to obtain a reliable estimate (third row) of the surface temperature response, as shown by *Hansen et al.* [2007]. All values in the table are rounded to two decimal places.

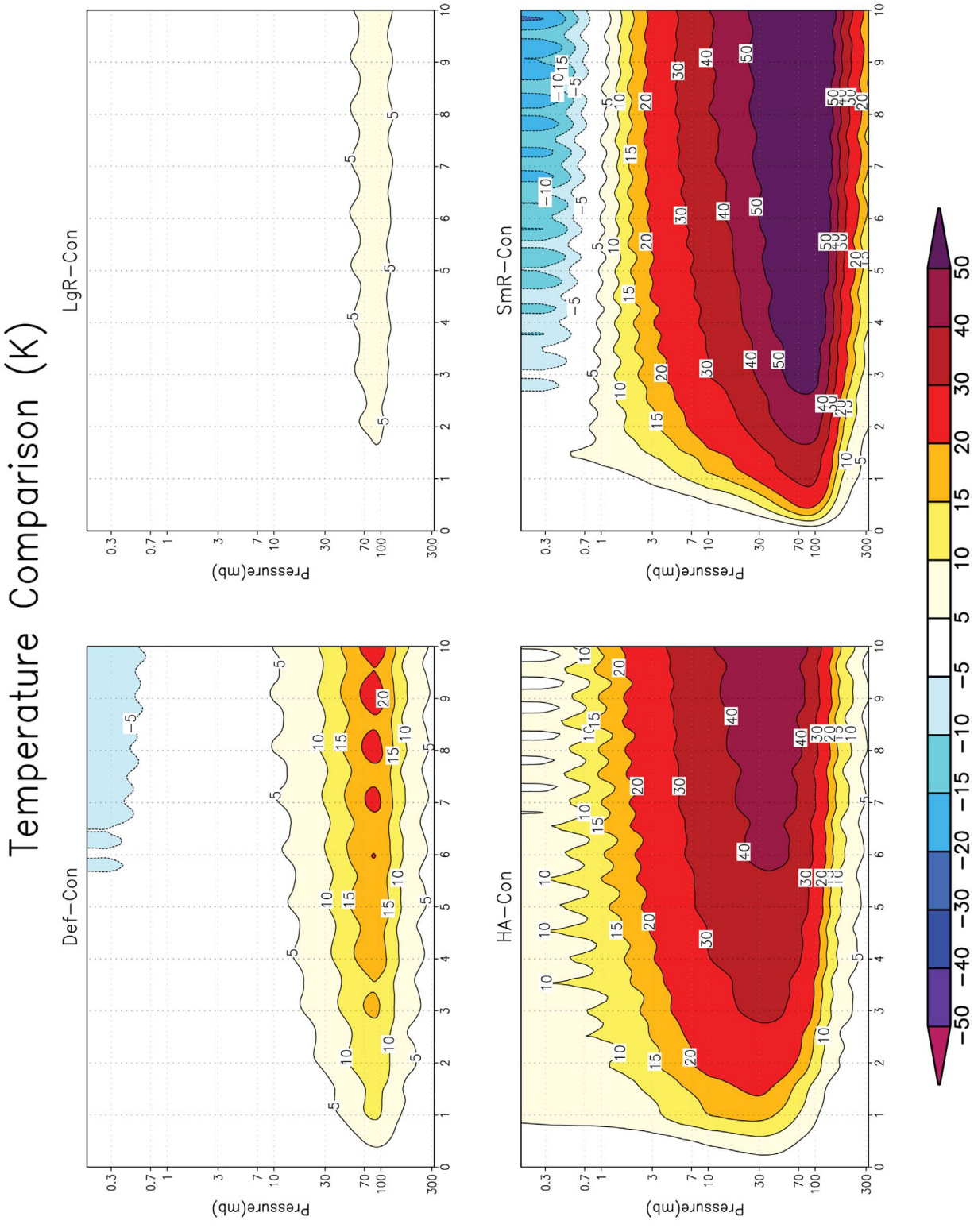

Figure 6. Stratospheric temperature anomalies for four of the ensembles, globally averaged.

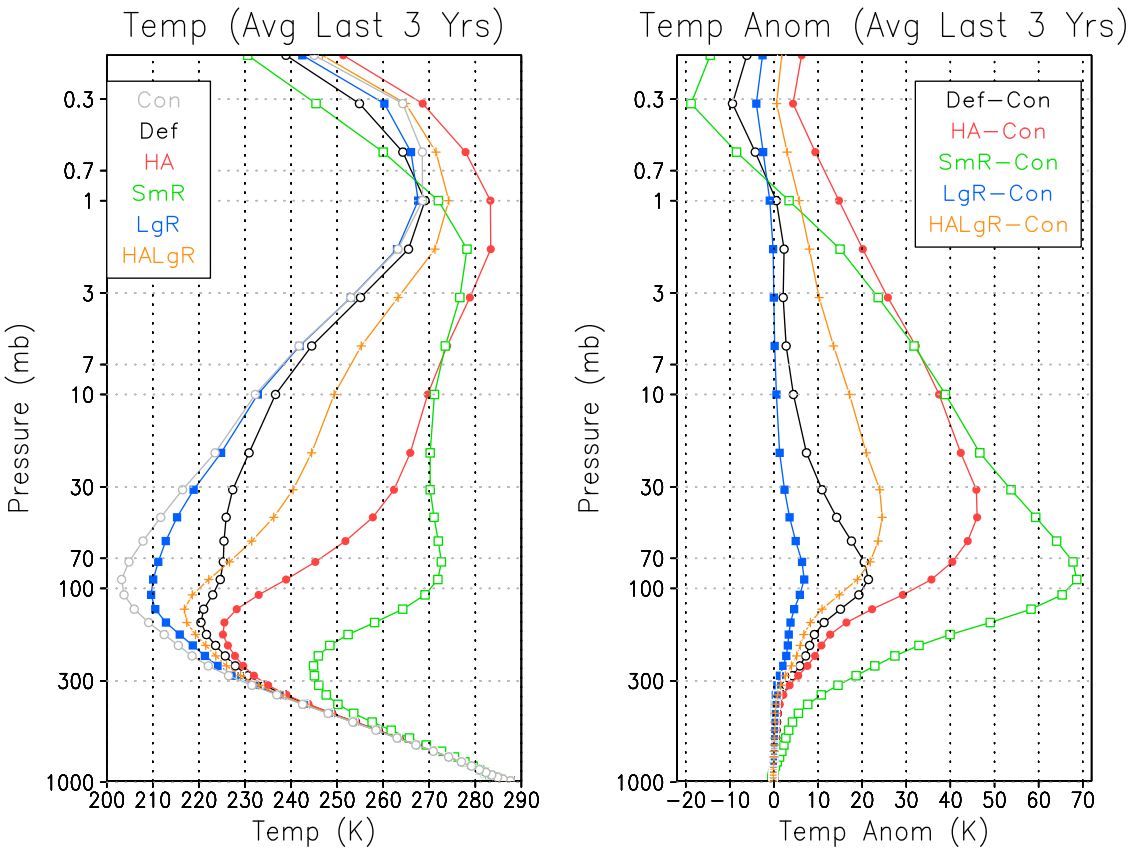

Figure 7. Vertical temperature profiles and anomalies (globally averaged) for the ensembles in Table 1. All values are averaged over the last three years of simulation (years 8–10).

chemistry of black carbon injection in great detail in reference to nuclear winter simulations. The model they use is far more detailed in terms of chemistry than ModelE2, but our simulations still capture the dominant processes that would lead to ozone loss. One is the Chapman mechanism [*Chapman*, 1930, 1942], described by the reaction

$$O_3 + O \rightarrow 2O_2$$

which accelerates with higher temperatures, and the ozone forming reaction

$$O + O_2 + M \rightarrow O_3 + M$$

which is slower for higher temperatures [*Groves et al.*, 1978]. Another is NO_x-catalyzed ozone destruction, which is also temperature sensitive:

$$NO + O_3 \rightarrow NO_2 + O_2$$
$$NO_2 + O \rightarrow NO + O_2$$

The third is an interaction with the HO_x cycle which results from increased water concentrations in the stratosphere (not pictured) due to warming of the tropical tropopause cold point:

$$OH + O_3 \rightarrow HO_2 + O_2$$
$$HO_2 + O_3 \rightarrow OH + 2O_2$$

[33] Figure 8 shows that experiment Def results in oscillating globally averaged ozone concentrations, with losses nearing 3% in austral summer and gains of nearly 4% in boreal summer. Spatial patterns show more complex behavior, with losses in the tropics, small gains in the subtropics, losses in the Arctic (most prominently in the spring), and gains in the Antarctic spring. Analyzing vertically resolved ozone mass, the stratospheric ozone layer shows a loss, but, similarly to *Mills et al.* [2008], our simulations show ozone recovery at lower altitudes in the tropics due to penetration of ultraviolet light to lower altitudes and consequent photodissociation of oxygen molecules [*Solomon et al.*, 1992]. In the Def ensemble, this recovery is enough to compensate for the stratospheric loss.

[34] Figure 9 shows that effects on ozone depend on aerosol size and altitude of injection. Ensembles Def and LgR show no global ozone loss, and even a slight increase in some seasons, which is due to the previously mentioned mechanism of low altitude ozone production, which dominates the small amounts of ozone loss in some seasons. HALgR, HA, and SmR all show large amounts of global ozone loss, with ensemble SmR reaching nearly 50% loss by the end of the ten-year simulation. Experiment HA shows similar results to the nuclear winter simulations of *Mills et al.* [2008], with globally averaged ozone losses of 27–30% in the tenth year of simulation. Excepting SmR, we again see a clear separation, in that ensembles involving injections at higher altitudes show more ozone loss than injections at lower altitudes.

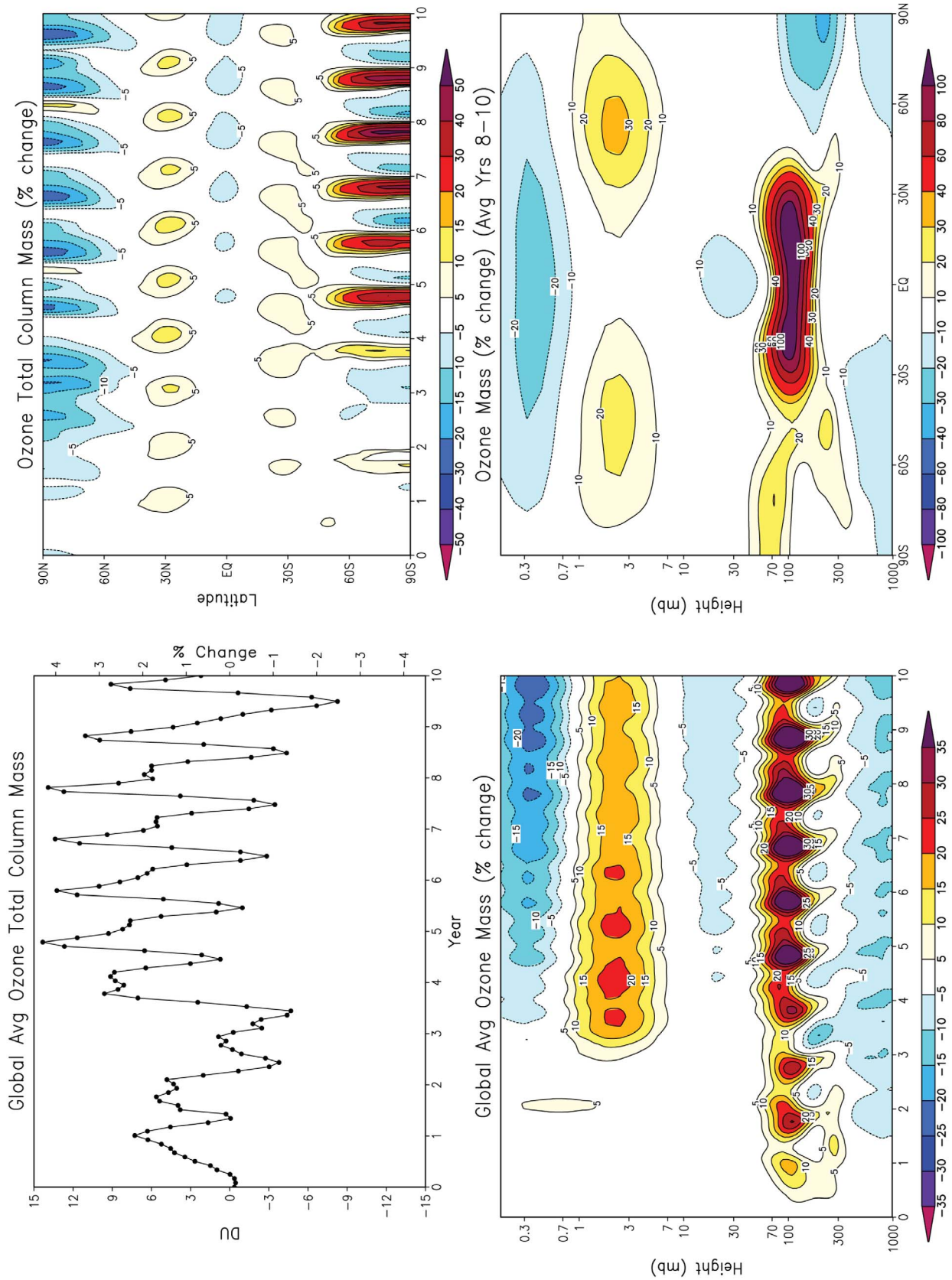
Ozone Total Column Mass (% change)
Latitude
90N
60N
30N
EQ
30S
60S
90S
Ozone Mass (% change) (Avg Yrs 8–10)
Height (mb)
Global Avg Ozone Total Column Mass
DU
% Change
Year
Global Avg Ozone Mass (% change)
Height (mb)

Figure 8

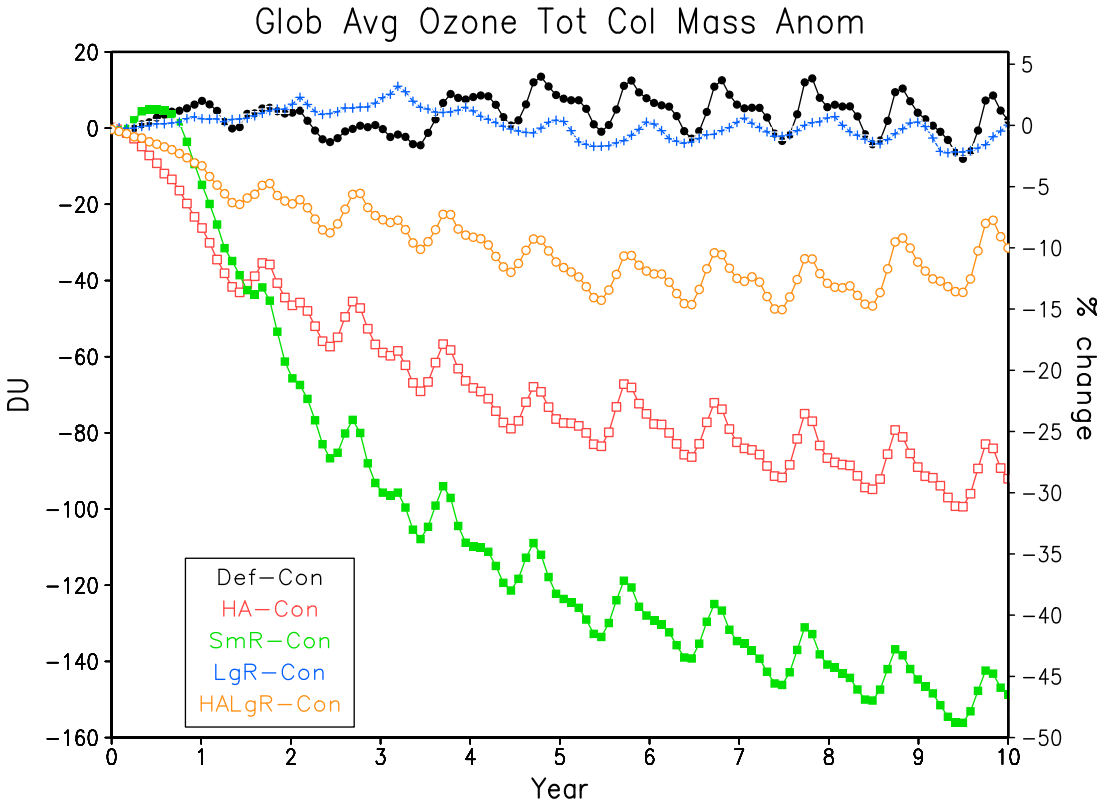

Figure 9. Globally averaged anomalies in total column ozone for each ensemble, given in Dobson Units (DU) and percent change.

[35] One of the features seen in Figure 8, which is also present in HALgR and SmR (not pictured) is Arctic ozone loss. Ozone destruction due to chlorofluorocarbon (CFC) emissions is a well known and publicized phenomenon [*Solomon*, 1999], without which the Antarctic ozone hole would not exist. However, in the presence of CFCs, the primary reason for concentrated ozone loss in the Antarctic is the circumpolar jet. The jet slows mixing with air from lower latitudes, so ozone loss that occurs in this area is not replenished rapidly through mixing with ozone-rich air. In turn, the jet slows horizontal heat transport, reducing compensation for radiative cooling in the polar night, allowing the pole to reach very cold temperatures. Additionally, heating outside the polar jet would assist in creating very cold temperatures over the Antarctic (by the thermal wind equation). These cold temperatures allow the formation of polar stratospheric clouds which serve as surfaces for ozone-destroying chlorine chemistry.

[36] Our results for stratospheric heating have strong potential for accelerating the Northern hemisphere polar jet, thus enhancing the Arctic ozone hole. Stratospheric heating after large volcanic eruptions is a well known phenomenon which causes dynamical effects, including strengthening of the polar jet in the Northern Hemisphere [*Stenchikov et al.*, 1998; *Robock*, 2000; *Shindell et al.*, 2001]. Therefore, the stratospheric heating from black carbon aerosol geoengineering, which is much greater than is found for large volcanic eruptions, would magnify this effect.

[37] Figure 10 shows anomalies in zonal wind resulting from the different geoengineering experiments and a control run climatology for comparison. LgR (not pictured) shows no apparent anomalies, and in Def, the anomalies are an increase in wind speed by 50% but are small compared to the other ensembles. HA and SmR show strengthening of winds by over a factor of two near both poles in summer and winter.

[38] Figure 11 shows climatologies (control ensemble) and anomalies over each pole in the seasonal cycle of total cloud fraction, which includes polar stratospheric cloud cover, in ensemble Def. The Arctic shows a reduction in upper-tropospheric cloud cover in the summer, which is consistent with heating from the aerosols, causing evaporation of clouds. In the winter, there is no sunlight, so heating from the aerosols is absent. Combining this with the strong jet seen in Figure 10 allows the Arctic stratosphere to cool in the winter (Figure 12), promoting Arctic PSC formation. Thus, we see evidence for the proposed mechanisms that would cause an Arctic ozone hole.

[39] Figure 8 also shows less Antarctic ozone loss in the austral spring, which is the time during which the ozone hole generally forms [*Solomon*, 1999]. Under normal circumstances, temperatures at this time are cold enough to allow PSCs to persist, but available sunlight initiates photodependent

Figure 8. Ozone anomalies that result from stratospheric geoengineering with black carbon aerosols in ensemble Def. (top left) Globally averaged ozone loss. (top right) Zonally averaged total column ozone anomalies. (bottom left) Globally averaged, showing a vertical profile of ozone mass concentrations. (bottom right) Averaged zonally and over the last three years of simulation (years 8–10), showing a vertical profile of ozone mass concentrations.

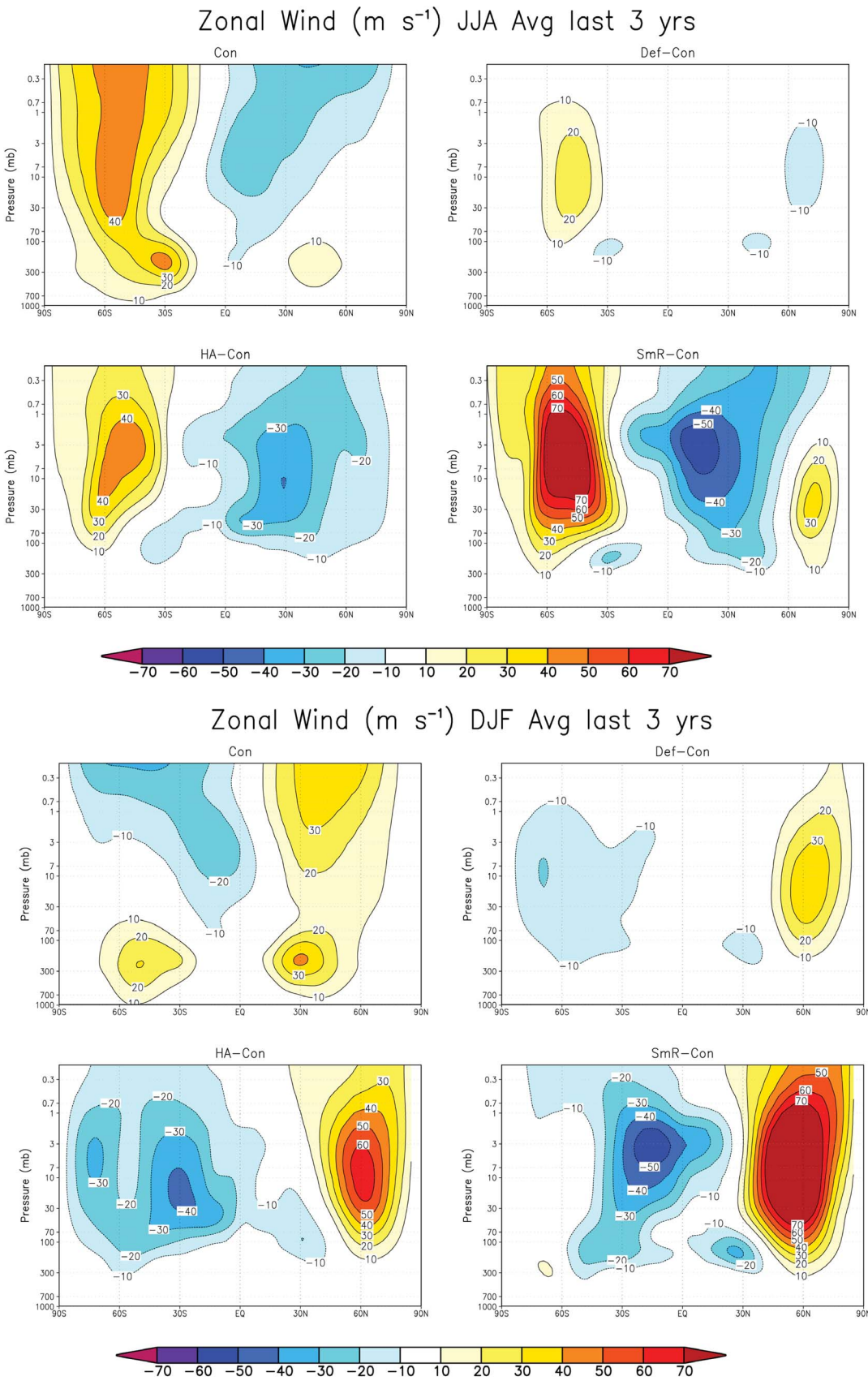
Zonal Wind (m s⁻¹) JJA Avg last 3 yrs
Con
Def−Con
HA−Con
SmR−Con
Zonal Wind (m s⁻¹) DJF Avg last 3 yrs
Con
Def−Con
HA−Con
SmR−Con
Pressure (mb)
0.3
0.7
1
3
7
10
30
70
100
300
700
1000
90S
60S
30S
EQ
30N
60N
90N
−70 −60 −50 −40 −30 −20 −10 10 20 30 40 50 60 70

Figure 10

chlorine chemistry which causes stratospheric ozone destruction. However, under geoengineering with black carbon aerosols, sunrise during the austral spring causes heating of the Antarctic stratosphere (Figure 12). PSCs cannot persist at these temperatures, leading to lower amounts of stratospheric cloud cover and consequently increased amounts of ozone over the background, a phenomenon which was also found by *Mills et al.* [2008] in their nuclear winter simulations.

[40] The amounts of ozone destruction due to chlorine chemistry presented in this study are perhaps not representative of the effects if geoengineering with black carbon aerosols were actually conducted. CFC concentrations have been declining, and the resulting effects on ozone by geoengineering with stratospheric aerosols will be less as time progresses [*Tilmes et al.*, 2008]. However, our results can potentially be used as an upper bound of the effects on ozone.

[41] One additional consequence of stratospheric heating by such large amounts is intrusive warming into the troposphere. Figure 13 shows globally averaged temperature anomalies for altitudes below 100 mb. All four ensembles show tropospheric warming. LgR expectedly shows the least warming, but anomalies of 0.25°C still extend down to 500 mb. The effects of a high altitude injection are seen in the comparison of Def and HA, in that tropospheric warming is lessened for higher altitude injections. SmR shows the most warming of the troposphere, with anomalies extending down to the boundary layer.

7. Practicality of Black Carbon Aerosol Geoengineering

[42] The next natural questions are, should policy makers desire to deploy black carbon geoengineering in the stratosphere, how would it be done, and how much would it cost? To answer these questions, we look at two methods of BC aerosol production: diesel combustion and carbon black.

[43] Soot production is a particularly sensitive marker of diesel exhaust [*Fruin et al.*, 2004]. Diesel combustion has the advantage of a vast infrastructure currently in place, including transportation and regulation, which would lend this technology particularly well to geoengineering purposes. Carbon black results from furnace combustion of heavy fuel oil in low oxygen [*Crump*, 2000]. It is generally an agglomeration of mostly elemental carbon particles, whereas black carbon aerosols often have adsorbed organic particles, depending upon the source of the emission [*Watson and Valberg*, 2001]. However, the mechanisms of formation of the two compounds are similar [*Medalia et al.*, 1983], so we can assume the particle density and refractive indices are similar. However, a typical radius of black carbon aerosol is approximately 0.1 μm [*Rose et al.*, 2006], while a typical carbon black agglomerate can have a diameter on the order of millimeters [*Gandhi*, 2005]. A larger diameter means a greatly increased fall speed as well as a reduced radiative efficiency, so the same mass of carbon black might be substantially less effective, or possibly ineffective, for geoengineering.

[44] The costs of these two different means are summarized in Table 5 and Figure 14. In Figure 14, we also include results from the calculations of *Robock et al.* [2009] for stratospheric sulfate aerosol geoengineering as a comparison.

7.1. Logistics and Costs of Using Diesel Fuel

[45] The black carbon emissions for heavy-duty diesel vehicles are approximately 1 g BC emitted per kg of fuel used [*Kirchstetter et al.*, 1999], but the highest emitting 10% of all heavy-duty diesel trucks produce 42% of black carbon emissions [*Ban-Weiss et al.*, 2009]. Assuming diesel engines could be tuned to produce 10 g black carbon per kg of fuel, the largest value reported by *Ban-Weiss et al.* [2009], and assuming an average density of 0.84 kg L^{-1} of diesel fuel [*T. W. Brown Oil Co., Inc.*, 1999], producing 1 Tg of black carbon would require combustion of 1.19×10^{11} L of diesel fuel, or approximately 10.8% of current worldwide production [*U. S. Energy Information Administration* (*EIA*), 2010a]. Refineries in the United States are operating at approximately 90% capacity [*EIA*, 2010b], so extrapolating this value worldwide implies geoengineering by combustion of diesel would require additional expansion of the current refining capacity, especially since this capacity is likely a theoretical maximum. We do not have estimates of cost for this expansion. We assume the cost of obtaining the oil, refining it into diesel, and transporting it to its desired destination, which would be the geoengineering deployment site, is included in the at-the-pump fuel cost. For each US $0.01 increase in the market price of diesel fuel, the annual cost of geoengineering increases by US $314 million.

[46] Industrial diesel engines are designed to run continuously at 100% capacity and need to be maintained relatively infrequently (Why we recommend used diesel generators, U. S. Power and Environment, 2010, http://www.uspowerco.com/articles/why_we_recommend_used_diesel_generators) (hereinafter USP&E, online article, 2010). As the central model for our calculations, we use specifications of the Caterpillar 3516B industrial engine (Caterpillar industrial wizard, 2010, http://industrialwizard.catmms.com/catwizards/industrialWizard/jsp/caterpillar.jsp.) (hereinafter, Caterpillar, online publication, 2010). Average costs for this particular engine are not available, but several auctions reported the sold price at US $395,000 (used), which we adopt as our price estimate. Assuming the engine is in operation for 2920 hours a year (365 days a year, 8 hours per day - the case for 24 hour per day operation is discussed in Table 5), this would require 75,100 engines at a capital cost of approximately US $30 billion. We do not include estimates of the cost of replacing the engines when they reach the end of their operational lifetime, but average diesel engine lifespans are in the range of 10–22 years [*MacKay & Co.*, 2003; *Lyon*, 2007].

[47] The maintenance costs are twofold: actual cost to maintain the engine and replacement engines to operate during the equipment's downtime. Maintenance requirements for the Caterpillar 3516B mean each engine will be inoperative 3.4% of the time (Caterpillar product operation and maintenance manuals (OMMS), 2010, http://safety.cat.com/cda/layout?m=133362&x=7.). To meet the required

Figure 10. Anomalies in zonal wind for three of the ensembles, as well as the control climatology (top left of each group). LgR is not included, as it showed few anomalies. Top four panels are for the boreal summer (JJA), and bottom four panels are for the austral summer (DJF). All values shown are averages of the last three years of simulation (years 8–10).

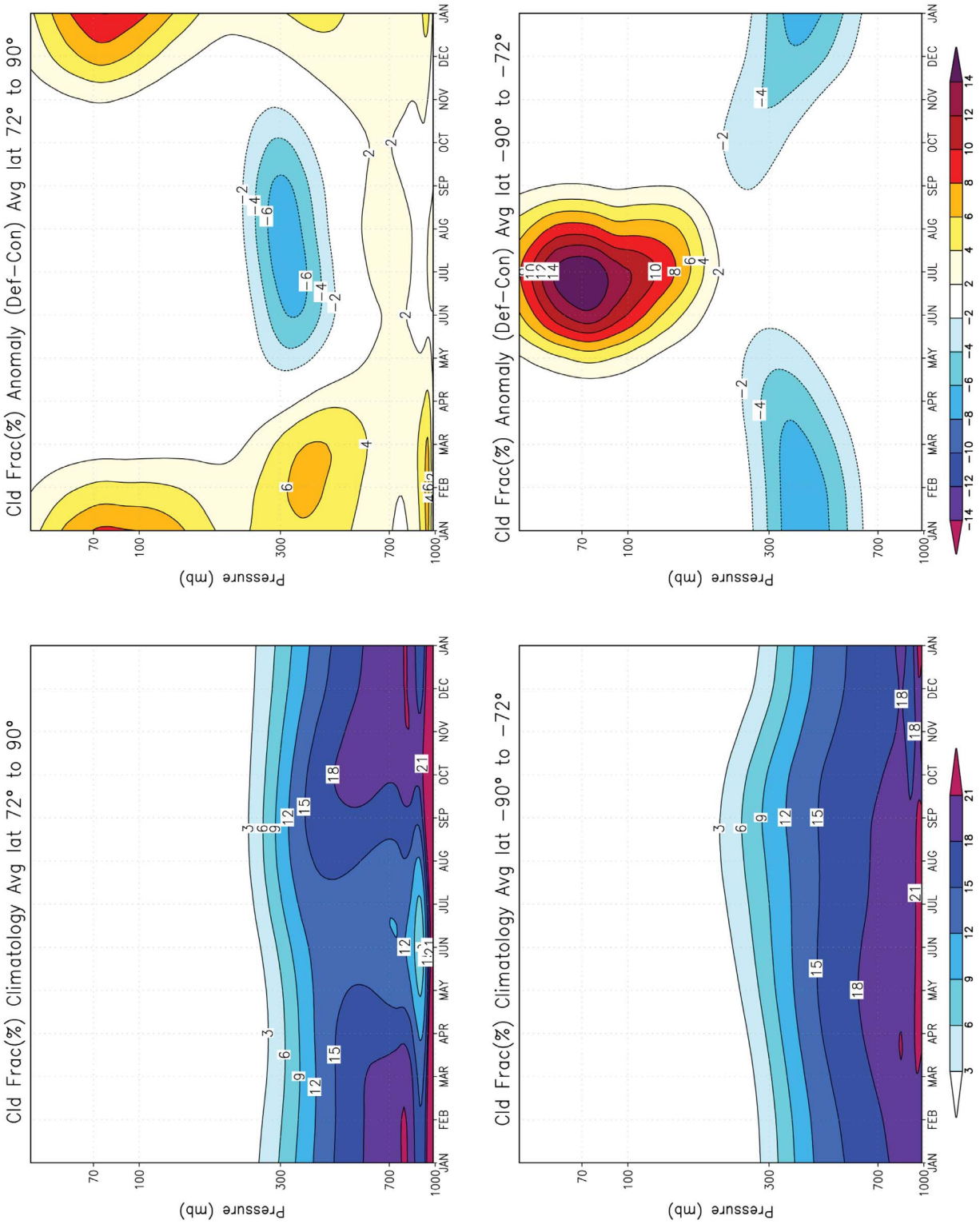

Figure 11. Climatology (control ensemble only) and climatological anomaly (Def-Con) in total cloud fraction over the poles (72–90 degrees in each hemisphere). Climatologies are averages over the last three years of simulation (years 8–10).

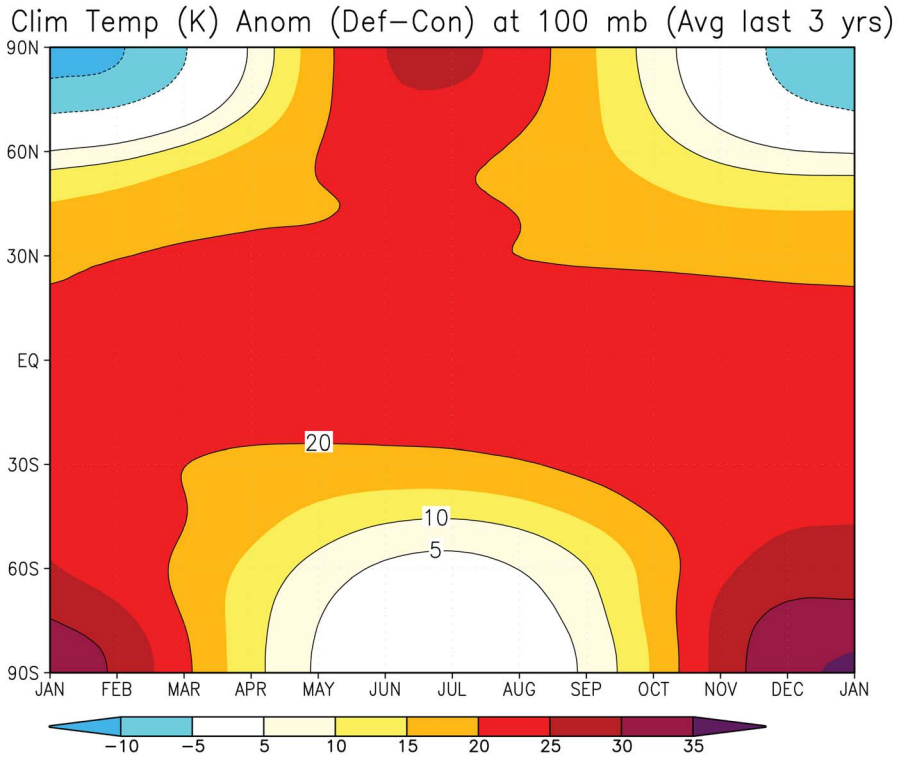

Figure 12. Seasonal climatology of temperature anomalies at 100 mb for ensemble Def, averaged over the last three years of simulation (years 8–10). Heating by the aerosols in the spring reduces cloud cover over the poles in the spring (Figure 11).

black carbon production rate, an additional 255 engines are required at a capital cost of US $100 million.

[48] Maintenance estimates for the Caterpillar G3520 industrial gas engine are approximately US $0.008 per kW-h, which is likely more expensive than maintaining a diesel engine (USP&E, online article, 2010). Using this as an upper bound, given that the 3516B runs at a maximum of 1492 kW of power generation (Caterpillar, online publication, 2010), the total annual maintenance cost is US $2.6 billion.

[49] A natural solution for getting the black carbon aerosols to the stratosphere is to place these diesel engines and diesel fuel in the cargo hold of airplanes and fly them to the stratosphere. *Robock et al.* [2009] evaluated several choices of aircraft that would be suitable for geoengineering (their cost estimates were similar to those of *McClellan et al.* [2010]), but we base our calculations here on the KC-10 Extender (Factsheets: KC-10 Extender, U.S. Air Force, 2010, http://www.af.mil/information/factsheets/factsheet.asp?fsID=109). It has a payload of 76,560 kg, a ceiling of 12.7 km, and a unit purchase price (2010 dollars) of US $116 million. This maximum altitude is only suitable for reaching the stratosphere at high latitudes, but because the aerosols self-loft, getting them to the upper troposphere is sufficient, resulting in rain-out of about 20% [*Mills et al.*, 2008; *Robock et al.*, 2007a; *Fromm et al.*, 2010].

[50] Each airplane is capable of carrying more than one engine, so we decompose our calculations into units consisting of an engine and 8 hours of diesel fuel. The 3516B engine weighs up to 8028 kg and can consume 4339.12 L of fuel in 8 hours for a total unit weight of 11,977.0 kg (Caterpillar marine and power systems, 2010, http://marine.cat.com/cat-3516B.). Each KC-10 Extender can hold 6 units per airplane, meaning 12,342 airplanes would be required at a total purchase price of US $1.4 trillion. *Curtin* [2003] gives an estimate of US $3.7 million in annual cost, based on 300 flying hours per year, for personnel, fuel, maintenance, modifications, and spare parts for the KC-135 airplane. As *Robock et al.* [2009] state, the KC-10 is a newer airplane and would likely be cheaper, so we use this value as an upper limit for our estimations. Scaling these maintenance costs, annual maintenance and personnel costs will be approximately US $36 million per plane, for a total annual operating cost of approximately US $450 billion.

[51] This combination results in a fixed cost of US $1.4 trillion and an operating cost of approximately US $540 billion. This is the cheapest of the methods shown in Table 5, which include calculations for the Caterpillar 3406C engine (Caterpillar, online publication, 2010), the KC-135 Stratotanker airplane (Factsheets: KC-135 Stratotanker, U.S. Air Force, 2010, http://www.af.mil/information/factsheets/factsheet.asp?fsID=110), and geoengineering in three 8-hour shifts per day instead of a single shift.

[52] The world gross domestic product (purchasing power parity) in 2009 was US $69.98 trillion [*Central Intelligence Agency*, 2010]. The initial investment for geoengineering would be 2.0% of worldwide GDP, with an additional 0.8% each year. *Stern* [2006] states the cost of climate change for 2–3°C of warming could be a permanent loss of up to 3% of GDP, so geoengineering with black carbon aerosols is slightly cheaper than the damage that would be caused by

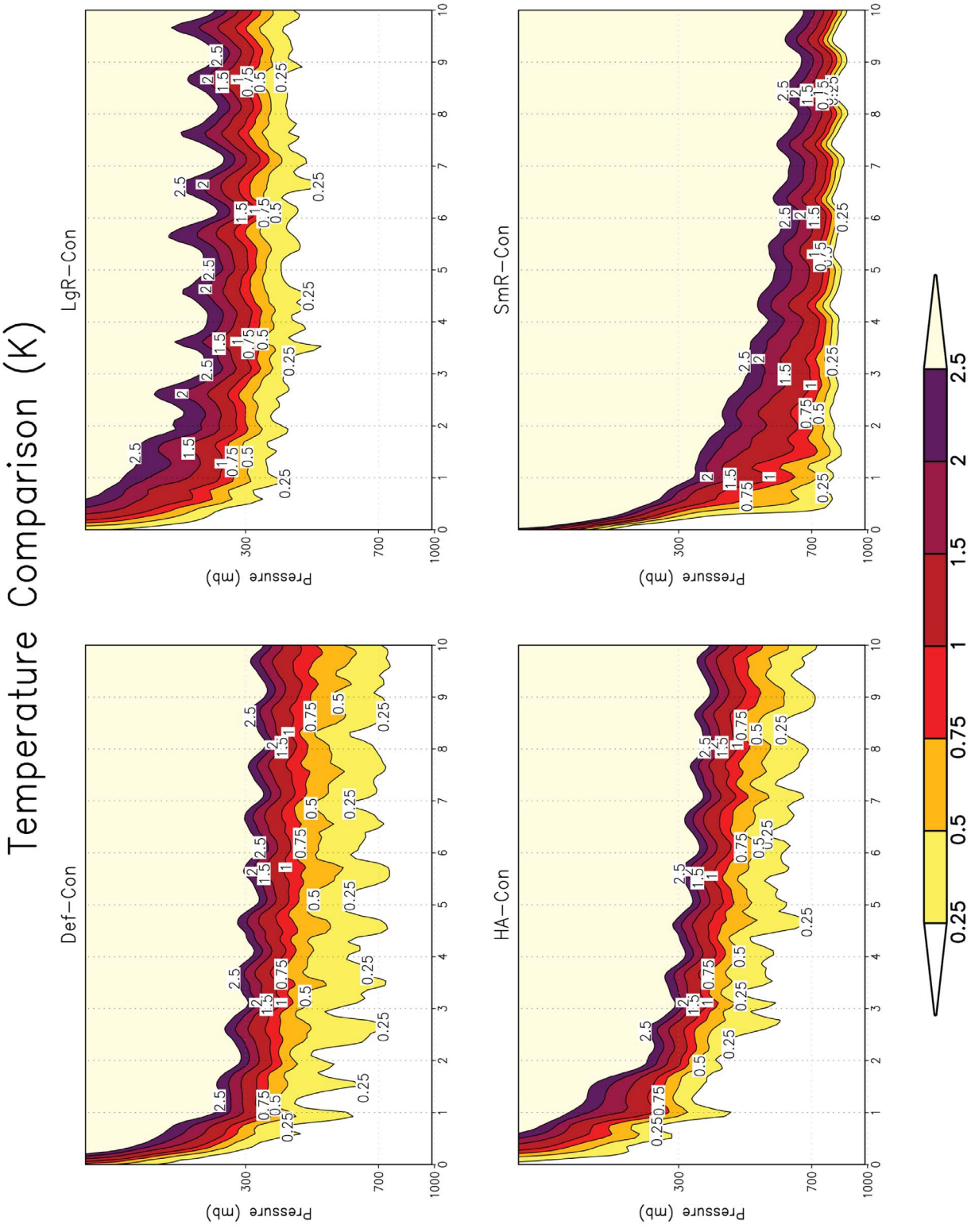

Figure 13. Globally averaged anomalies in tropospheric temperature for four of the geoengineering ensembles.

Table 5. Fixed (One-Time) and Annual Costs for Geoengineering by Combustion of Diesel Fuel for Each Considered Combination of Diesel Engine, Airplane, and Daily Shift Number[a]

	2920 Hours per Year		8760 Hours per Year	
Engine/Airplane	Fixed	Annual	Fixed	Annual
3516B, KC-135	US $1300 B	US $990 B	US $460 B	US $2800 B
3516B, KC-10	US $1400 B	US $540 B	US $510 B	US $1400 B
3406C, KC-135	US $1600 B	US $1200 B	US $550 B	US $3400 B
3406C, KC-10	US $1800 B	US $650 B	US $600 B	US $1700 B

[a]Included in the annual costs are an estimate of fuel consumption with an at-the-pump price of US $3.00 per gallon, for a total of US $94.3 billion. Values reported are in billions of dollars (B) and are rounded to two significant digits.

climate change and is vastly more expensive than geoengineering with sulfate aerosols [*Robock et al.*, 2009]. *Intergovernmental Panel on Climate Change* (*IPCC*) [2007] calculates that mitigation to reach a stabilization of 535–590 ppm CO_2-eq would result in a GDP reduction by 0.2–2.5%, with a median reduction of 0.6% and an annual reduction of GDP growth rate by less than 0.1%. Compared to the cost of black carbon geoengineering by diesel fuel combustion, mitigation either costs the same or is cheaper by as much as an order of magnitude.

[53] The largest source of cost in this method is using airplanes to fly the diesel fuel and engines up to the stratosphere. If the black carbon aerosols were produced on the ground, collected, and then flown into the stratosphere to be dispersed, the fixed costs could be reduced to about US $31 billion, and the annual costs could be reduced to about US $97 billion [*Robock et al.*, 2009].

[54] Thus far we have not considered the potential benefit of generation of a large amount of electricity from diesel fuel combustion. Using the Caterpillar 3516B engine would create approximately 330 TW-h of energy per Tg of BC aerosols produced, which could possibly be used to power the airplanes, reducing the associated costs and resources of operating the fleet. For comparison, in 2008, the worldwide energy consumption was approximately 132,000 TW-h [*British Petroleum*, 2009].

7.2. Logistics and Costs of Using Carbon Black

[55] Carbon black feedstock is produced from fractional distillation of petroleum and is generally extracted as a heavy or residual fuel oil [*Dow Chemical Company*, 2010a, 2010b; *International Carbon Black Association*, 2004]. The yield of carbon black from the oil furnace process is 35–65% per mass of residual fuel oil, depending upon the chosen feedstock and the desired particle size, with smaller particles resulting in lower yields [*U.S. Environmental Protection Agency* (*EPA*), 1995]. Small particles are more efficient for geoengineering, so we use the lowest value in this range. Assuming an average density of carbon black feedstock of 1.08 kg L^{-1} [*Dow Chemical Company*, 2010b] and that suitable feedstock (residual fuel oil) comprises approximately 8% of refinery yields [*EIA*, 2010b], producing 1 Tg of carbon black will require 3.18×10^{10} L of oil, or an additional 0.8% of current worldwide production [*EIA*, 2010b].

[56] Available furnace black production capacity in the United States (1998) is 1.6×10^9 kg of carbon black, more

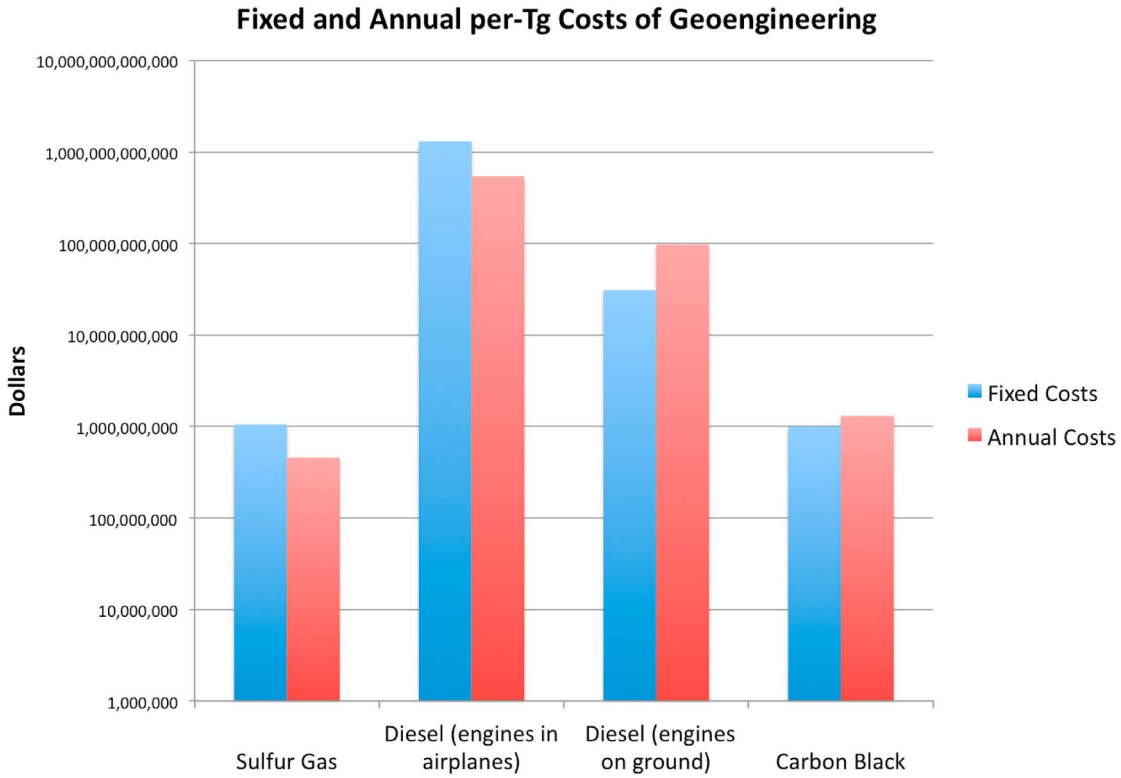

Figure 14. Fixed (one-time) and annual per-Tg costs of stratospheric geoengineering with black carbon aerosols. Sulfur gas calculations are repeated from *Robock et al.* [2009] and are included for comparison.

Table 6. Significant Emissions Factors for Diesel Fuel Combustion and Carbon Black Production[a]

Emissions Factor	Diesel Fuel (kg/Tg BC)	Carbon Black (kg/Tg BC)
CO_2	3.2×10^{11}	
NO_x	8.5×10^9	
CO	1.8×10^9	1.4×10^6
organics (exhaust)	6.8×10^8	
organics (crankcase)	1.9×10^7	
PM-10	6.0×10^8	
SO_x	5.7×10^8	
aldehydes	1.4×10^8	
H_2S		3×10^4
CS_2		3×10^4
OCS		1×10^4
CH_4		2.5×10^4
C_2H_2		4.5×10^4

[a]Emissions factors for diesel fuel are from *EPA* [1996, 2005] and for carbon black from *EPA* [1995]. All emissions factors are in total number of kg emitted for producing 1 Tg of black carbon aerosol (diesel fuel combustion) or carbon black. 95% of all carbon black is created by the furnace black process [*Crump*, 2000], so we use those emissions factors here. Only emissions factors which were deemed to be significant products are included.

than sufficient to produce 1 Tg [*Crump*, 2000]. Annual production costs for all carbon black produced in the United States (1998) was US $625 million, or approximately US $0.33 per kg, with the finest grade having a 1998 cost of approximately US $1.03 per kg. Therefore, using current infrastructure, producing 1 Tg of carbon black would cost approximately US $1 billion.

[57] The costs of ferrying 1 Tg of carbon black to the stratosphere are similar to those reported in *Robock et al.* [2009]. The cheapest transportation option has fixed costs of US $1 billion and annual costs of about US $320 million. Including the cost of manufacturing the carbon black, the total per-Tg cost of geoengineering with carbon black is US $1 billion fixed and US $1.3 billion annually. We do not include the cost of transporting the carbon black to the geoengineering site in these estimates.

7.3. Emissions Factors

[58] Table 6 summarizes the various emission factors for the most abundant products of aerosol production, some of which we examine in more detail.

[59] Carbon dioxide, the chief contributor to climate change, is the largest emissions factor in Table 6 [*IPCC*, 2007]. The total worldwide emissions of CO_2 are approximately 30 Pg of CO_2 per year [*International Energy Agency*, 2011], so this would constitute an additional 1.1% of emissions. The additional CO_2 produced from jet fuel combustion as part of the geoengineering process would be less than 1% of current aviation emissions, which are already only 2–3% of current worldwide emissions (Enviro Aero, Beginner's Guide to Aviation Biofuels, 2009, http://www.enviro.aero/biofuels).

[60] Diesel combustion produces NO_x from high temperature dissociation of ambient nitrogen [*EPA*, 1996]. Creating 1 Tg of black carbon aerosols from diesel combustion would produce 8.5 Tg of NO_x. Total worldwide NO emissions in 1990 were 49.6 Tg [*Stevenson et al.*, 2004], so this source of NO_x would be an additional 17%. NO_x is an effective catalyst for destruction of stratospheric ozone [*Crutzen*, 1970]. This mechanism competes with reactions between other species, depending upon altitude [*Finlayson-Pitts and Pitts*, 2000]. Based on an experiment by *Stolarski et al.* [1995] simulating ozone destruction from a stratospheric fleet of high speed civil transport aircraft and extrapolating from a linear fit to their results, we roughly estimate that combustion of diesel fuel for geoengineering could cause a −10 to −3% change in total ozone column due to NO_x alone.

[61] CO is by far the predominant emissions factor of carbon black manufacturing, although the CO emissions can be reduced by up to 99.8 percent by controlling with CO boilers, incinerators, or flares [*EPA*, 1995]. Without these controls, producing 1 Tg of carbon black would result in the emission of 1.4×10^6 kg of CO. Diesel combustion would result in a larger amount of 1.8×10^9 kg of CO. Carbon monoxide is naturally produced at a rate of 5×10^{12} kg annually in the troposphere [*Weinstock and Niki*, 1972], so the additional CO from producing this large amount of aerosols would be negligible. The stratosphere is a natural sink for carbon monoxide, due to reaction with the hydroxyl radical [*Pressman and Warneck*, 1970], so we anticipate this emissions factor would not cause any noticeable adverse effects.

[62] Sulfur compounds resulting from diesel fuel combustion are due to sulfur content of the fuel. During the combustion process, nearly all of the sulfur is oxidized to SO_2, which is a precursor to sulfate aerosols [*EPA*, 1996]. Using the emissions factor given in Table 6, creating 1 Tg of black carbon aerosols would result in the production of approximately 0.57 Tg of SO_2, which would cause small climate effects but would still impact the planetary radiation budget [*Robock et al.*, 2008; *Kravitz and Robock*, 2011; *Solomon et al.*, 2011]. It is an insufficient amount to produce damaging acid rain [*Kravitz et al.*, 2009]. Since the reporting of the year 1996 emissions factors given in Table 6, ultra-low sulfur diesel has been introduced to the market and is the only readily available diesel fuel in the United States [*EPA*, 2009], so this emissions factor would likely be lower than the values reported here. The chemistry effects of this increase in SO_x may not be trivial, especially when considering the effects on ozone. Simulations of 2 Tg a^{-1} injections of S into the stratosphere showed a delay in the recovery of the ozone hole by approximately 30 years [*Tilmes et al.*, 2009], suggesting the additional SO_x from our diesel fuel combustion calculations has the potential to cause ozone destruction.

[63] Methane is a powerful greenhouse gas, 23 times more effective than CO_2 on a 100-year timescale [*IPCC*, 2007]. From the emissions factor reported in Table 6, producing 1 Tg of carbon black would result in the production of 2.5×10^4 kg of methane, or an increase in atmospheric concentrations by much less than 1 part per trillion. Current concentrations of methane are on the order of 1 ppm [*IPCC*, 2007], so this is a negligible contribution.

8. Discussion and Conclusions

[64] The radiative effectiveness at causing surface cooling depends strongly upon the aerosol size and altitude of injection. According to our simulations, with the exception of using small aerosols, possibly smaller than can be reasonably produced in large quantities, altitude of injection appears to be more important than aerosol size in determining the climate impacts of black carbon geoengineering.

[65] The climate effects of this means of geoengineering have the potential to be severe, including stratospheric heating, ozone loss, and circulation changes. However, the degree of climate effects presented in this study are likely exaggerated. The values of cooling in Table 4 are quite large and are well in excess of any reasonable perturbation that would be desired for geoengineering as a means of countervailing increasing surface air temperatures due to anthropogenic CO_2. Future studies of black carbon geoengineering would likely use considerably less mass than 1 Tg BC a^{-1}, possibly by several orders of magnitude.

[66] However, not all impacts of geoengineering will scale linearly with amount. Although the radiative impacts of aerosols are approximately linear with mass loading (assuming no change in the aerosol microphysical properties) [*Hansen et al.*, 2005; *Ricke et al.*, 2010], the chemical effects are certainly nonlinear. *Ross et al.* [2010] simulated stratospheric injections of black carbon with a mass loading of 2600 tons, approximately 500 times lower than the equilibrium loading for ensemble Def, yet showed tropical increases in ozone by up to 4% and losses in the Antarctic by 15%. These results imply that although reducing the amount of geoengineering can reduce the radiative impacts approximately linearly, the effects on chemistry and ozone require a great deal of further investigation.

[67] One particularly concerning result from our simulations is warming of the upper troposphere. The Tibetan Plateau has an altitude of approximately 500 mb [*Zhisheng et al.*, 2001], well within the range of atmospheric warming, inviting the possibility of enhancing melting of glaciers. Not only would this create a positive feedback causing further warming, as melting of the glaciers will reduce the albedo of the Tibetan Plateau, but it would also reduce the available fresh water to all of the population centers downriver of the plateau, including China and India. In this sense, stratospheric geoengineering with black carbon could be catastrophic, although more analysis is needed to exactly determine the degree of deglaciation and the resulting impacts. Tropospheric warming, as was seen in Figure 13, also causes stabilization of the troposphere, which would have significant consequences for formation of deep convection, as well as cloud systems in general, suggesting serious implications for the hydrologic cycle.

[68] The logistics of geoengineering with black carbon aerosols via diesel combustion appear prohibitive, even if the amount of aerosol needed was an order of magnitude less. Of the means we discussed in Section 7.2, the costs are large, and the oil requirements would strain the current production market and refining capacity. Using a different source for the aerosol, such as carbon black, is similar in cost to using sulfate aerosols [*Robock et al.*, 2009]. However, whether carbon black can be ground into particles that are small enough to be useful for geoengineering has yet to be determined.

[69] It is likely that geoengineering with black carbon aerosols has risks that are too great to make it a viable option for deployment. However, this study still has use as part of a spectrum. Sulfate aerosols, which have received the most attention in the study of stratospheric geoengineering, are excellent scatterers, and black carbon is an excellent absorber. Therefore, any choice of aerosol, be it natural or engineered, can be seen as lying on a spectrum between sulfate and black carbon in terms of the relative fractions of scattered and absorbed light.

[70] This study invites a great deal of future work. One of the major shortcomings of this study is the use of fixed sea surface temperatures. Although this is very useful and a standard method in CCMVal simulations [*SPARC CCMVal*, 2010] to isolate the stratospheric response, this does not allow us to assess ocean heat uptake, which modulates surface air temperature and affects circulation patterns. It also severely hampers our ability to assess effects on the hydrologic cycle and the cryosphere. Of particular importance is the "dirty snow effect" which describes a decrease in albedo of fresh snow as soot deposits onto it [*Vogelmann et al.*, 1988]. Additionally, our discussion of cloud cover is limited to polar stratospheric clouds, as our inability to accurately assess the hydrologic cycle carries through to tropospheric cloud cover.

[71] Changes in ozone concentrations and the polar vortices have links to air temperature and circulation which depend upon ocean temperature. These effects cannot be considered in our study, although the bulk of impacts on these two quantities is due to the large amount of stratospheric heating seen in our simulations, the magnitude of which would likely overwhelm any secondary effects.

[72] Some of the chemical effects we described would benefit from more thorough analysis. Excellent treatments of the chemical implications of geoengineering with stratospheric aerosols have been performed [*Tilmes et al.*, 2008; *Heckendorn et al.*, 2009]. Although these studies involved sulfate aerosols, many similar considerations would also apply to black carbon aerosols [*Mills et al.*, 2008; *Ross et al.*, 2010]. Additionally, the sensitivity of our results to aerosol size implies that unanticipated reductions in aerosol size due to chemistry or other potential influences could present serious problems.

[73] One large source of uncertainty in our study is the interactions of the aerosols with clouds. Adding absorbing interstitial aerosols to clouds would almost certainly alter their radiative properties, causing them to absorb more solar radiation. The absorption of solar radiation by black carbon is potent in a multiple scattering environment where the probability of photon interaction with the BC aerosol is greatly enhanced. While such absorption would probably assist in reducing the surface temperature by reducing shortwave radiation, the temperature of the atmospheric column would likely be substantially increased and longwave downwelling increased. This would likely reduce the efficiency of black carbon geoengineering in regions with significant cloud cover. Similarly, one may quickly deduce that this mechanism could be catastrophic in the marine stratus belts where a small amount of warming in the cloud decouples it from the underlying ocean that supplies the vapor which maintains the cloud system, which in turn could cause evaporation of the clouds. This aspect would benefit from a modeling experiment in which significant concentrations of absorbing aerosols were added to clouds, giving photons an opportunity to be absorbed in a multiple scattering environment.

[74] And finally, an important consideration is the effects of geoengineering on health. The impacts are numerous, but of particular note is the toxicity of the aerosols once they have descended into the troposphere [*Baan et al.*, 2006; *Center for Disease Control*, 1999]. Moreover, the additional

ultraviolet radiation that would reach the surface due to ozone loss would be detrimental to human health and large parts of the biosphere [*Hutchinson et al.*, 1985; *Madronich et al.*, 1998; *Molina et al.*, 2000].

[75] The study of black carbon geoengineering is useful in understanding the climate response to a spectrum of different aerosol properties. However, due to the numerous, potentially catastrophic side effects, it is likely not viable itself as a means of modifying the climate.

[76] **Acknowledgments.** We thank Barbara Turpin, Ken Caldeira, and Anthony Broccoli for comments, as well as the reviewers for helpful suggestions. Model development and computer time at NASA Goddard Space Flight Center are supported by National Aeronautics and Space Administration climate modeling grants. The work of Kravitz and Robock is supported by NSF grant ATM-070452.

References

Baan, R., K. Straif, Y. Grosse, B. Secretan, F. El Ghissassi, and V. Cogliano (2006), Carcinogenicity of carbon black, titanium dioxide, and talc, *Lancet Oncol.*, *7*(4), 295–296, doi:10.1016/S1470-2045(06)70651-9.

Ban-Weiss, G. A., M. M. Lunden, T. W. Kirchstetter, and R. A. Harley (2009), Measurement of black carbon particle number emission factors from individual heavy-duty trucks, *Environ. Sci. Technol.*, *43*(5), 1419–1424, doi:10.1021/es8021039.

Ban-Weiss, G. A., L. Cao, G. Bala, and K. Caldeira (2012), Dependence of climate forcing and response on the altitude of black carbon aerosols, *Clim. Dyn.*, *38*, 897–911, doi:10.1007/s00382-011-1052-y.

British Petroleum (2009), BP statistical review of world energy June 2009, report, 48 pp., London. [Available at http://www.bp.com/liveassets/bp_internet/globalbp/globalbp_uk_english/reports_and_publications/statistical_energy_review_2008/STAGING/local_assets/2009_downloads/statistical_review_of_world_energy_full_report_2009.pdf.]

Center for Disease Control (1999), Elemental carbon (diesel particulate): Method 5040, Issue 3 (Interim), in *NIOSH Manual of Analytical Methods*, 4th rev. ed., pp. 5040-1–5040-9, Cent. for Disease Control, Washington, D. C. [Available at http://www.cdc.gov/niosh/docs/2003-154/pdfs/5040f3.pdf.]

Central Intelligence Agency (2010), *The World Factbook 2010*, Potomac Books, Washington, D. C. [Available at https://www.cia.gov/library/publications/the-world-factbook/geos/xx.html.]

Chapman, S. (1930), On ozone and atomic oxygen in the upper atmosphere, *Philos. Mag.*, *10*, 369–383.

Chapman, S. (1942), The photochemistry of atmospheric oxygen, *Rep. Prog. Phys.*, *9*, 92–100, doi:10.1088/0034-4885/9/1/310.

Chylek, P., G. Videen, D. Ngo, R. G. Pinnick, and J. D. Klett (1995), Effect of black carbon on the optical properties and climate forcing of sulfate aerosols, *J. Geophys. Res.*, *100*, 16,325–16,332.

Crump, E. L. (2000), Economic impact analysis for the proposed carbon black manufacturing NESHAP, *EPA-452/D-00-003*, 16 pp., Environ. Prot. Agency, Washington, D. C. [Available online at http://www.epa.gov/ttnecas1/regdata/EIAs/carbonblackeia.pdf.]

Crutzen, P. J. (1970), The influence of nitrogen oxides on the atmospheric ozone content, *Q. J. R. Meteorol. Soc.*, *96*(408), 320–325, doi:10.1002/qj.49709640815.

Crutzen, P. J. (2006), Albedo enhancement by stratospheric sulfur injections: A contribution to resolve a policy dilemma?, *Clim. Change*, *77*, 211–219, doi:10.1007/s10584-006-9101-y.

Curtin, N. P. (2003), Information on Air Force serial refueling tankers, testimony before the Subcommittee on Projection Forces, Committee on Armed Services, House of Representatives, *Rep. GAO-03-938T*, 8 pp., Gov. Account. Off., Washington, D. C. [Available at http://www.gao.gov/new.items/d03938t.pdf.]

Dow Chemical Company (2010a), Carbon black feed safety data sheet, report, 8 pp., Midland, Mich. [Available at http://www.dow.com/PublishedLiterature/dh_03df/0901b803803df6d8.pdf.]

Dow Chemical Company (2010b), Carbon black feedstock product safety assessment, report, 6 pp., Midland, Mich. [Available online at http://www.dow.com/PublishedLiterature/dh_0538/0901b80380538c53.pdf.]

Ferraro, A. J., E. J. Highwood, and A. J. Charlton-Perez (2011), Stratospheric heating by potential geoengineering aerosols, *Geophys. Res. Lett.*, *38*, L24706, doi:10.1029/2011GL049761.

Finlayson-Pitts, B. J., and J. N. Pitts Jr. (2000), *Chemistry of the Upper and Lower Atmosphere: Theory, Experiments, and Applications*, 969 pp., Academic, San Diego, Calif.

Fromm, M., et al. (2010), The untold story of pyrocumulonimbus, *Bull. Am. Meteorol. Soc.*, *91*, 1193–1209, doi:10.1175/2010BAMS3004.1.

Fruin, S. A., A. M. Winer, and C. E. Rodes (2004), Black carbon concentrations in California vehicles and estimation of in-vehicle diesel exhaust particulate matter exposures, *Atmos. Environ.*, *38*, 4123–4133, doi:10.1016/j.atmosenv.2004.04.026.

Gandhi, B. (2005), Reassessment of one exemption from the requirement of a tolerance for carbon black, report, 9 pp., Environ. Prot. Agency, Washington, D. C. [Available online at http://www.epa.gov/opprd001/inerts/carbonblack.pdf.]

Govindasamy, B., and K. Caldeira (2000), Geoengineering Earth's radiation balance to mitigate CO_2-induced climate change, *Geophys. Res. Lett.*, *27*(14), 2141–2144, doi:10.1029/1999GL006086.

Groves, K. S., S. R. Mattingly, and A. F. Tuck (1978), Increased atmospheric carbon dioxide and stratospheric ozone, *Nature*, *273*, 711–715.

Hansen, J., et al. (2005), Efficacy of climate forcings, *J. Geophys. Res.*, *110*, D18104, doi:10.1029/2005JD005776.

Hansen, J., et al. (2007), Climate simulations for 1880–2003 with GISS modelE, *Clim. Dyn.*, *29*, 661–696, doi:10.1007/s00382-007-0255-8.

Hansen, J., R. Ruedy, M. Sato, and K. Lo (2010), Global surface temperature change, *Rev. Geophys.*, *48*, RG4004, doi:10.1029/2010RG000345.

Heckendorn, P., D. Weisenstein, S. Fueglistaler, B. P. Luo, E. Rozanov, M. Schraner, L. W. Thomason, and T. Peter (2009), The impact of geoengineering aerosols on stratospheric temperature and ozone, *Environ. Res. Lett.*, *4*, 045108, doi:10.1088/1748-9326/4/4/045108.

Hutchinson, T. C., M. A. Harwell, W. P. Cropper, and H. D. Grover (1985), Additional potential effects of nuclear war on ecological systems, in *Environmental Consequences of Nuclear War*, edited by M. A. Harwell and T. C. Hutchinson, pp. 174–184, John Wiley, Hoboken, N. J.

Intergovernmental Panel on Climate Change (IPCC) (2007), *Climate Change 2007: the Fourth Assessment Report of the Intergovernmental Panel on Climate Change*, 996 pp., Cambridge Univ. Press, Cambridge, UK.

International Carbon Black Association (2004), Carbon black user's guide: Safety, health, and environmental information, report, 11 pp., Boston, Mass. [Available at http://www.carbon-black.org/carbonblackuserguide.pdf.]

International Energy Agency (2011), CO_2 emissions from fuel combustion: Highlights, 134 pp., Paris. [Available online at http://www.iea.org/co2highlights/CO2highlights.pdf.]

Keith, D. W. (2010), Photophoretic levitation of engineered aerosols for geoengineering, *Proc. Natl. Acad. Sci. U. S. A.*, *107*(38), 16,428–16,431, doi:10.1073/pnas.1009519107.

Kirchstetter, T. W., R. A. Harley, N. M. Kreisberg, M. R. Stolzenburg, and S. V. Hering (1999), On-road measurement of fine particle and nitrogen oxide emissions from light and heavy duty motor vehicles, *Atmos. Environ.*, *33*(18), 2955–2968, doi:10.1016/S1352-2310(99)00089-8.

Koch, D. (2001), Transport and direct radiative forcing of carbonaceous and sulfate aerosols in the GISS GCM, *J. Geophys. Res.*, *106*, 20,311–20,332.

Kravitz, B., and A. Robock (2011), The climate effects of high latitude eruptions: The role of the time of year, *J. Geophys. Res.*, *116*, D01105, doi:10.1029/2010JD014448.

Kravitz, B., A. Robock, L. Oman, G. Stenchikov, and A. B. Marquardt (2009), Sulfuric acid deposition from stratospheric geoengineering with sulfate aerosols, *J. Geophys. Res.*, *114*, D14109, doi:10.1029/2009JD011918.

Kravitz, B., A. Robock, O. Boucher, H. Schmidt, K. Taylor, G. Stenchikov, and M. Schulz (2011), The Geoengineering Model Intercomparison Project (GeoMIP), *Atmos. Sci. Lett.*, *12*, 162–167, doi:10.1002/asl.316.

Lane, L., K. Caldeira, R. Chatfield, and S. Langhoff (2007), Workshop report on managing solar radiation, *NASA/CP-2007-214558*, 31 pp., NASA Goddard Space Flight Cent., Greenbelt, Md.

Lyon, S. (2007), The Massachusetts 2002 diesel particulate matter inventory, report, 123 pp., Mass. Dep. of Environ. Prot., Boston. [Available online at http://www.mass.gov/dep/air/priorities/02dslinv.pdf.]

MacKay & Co. (2003), America's fleet remains strong, *Constr. Equip.*, *August 2003*, 10 pp.

Madronich, S., R. L. McKenzie, L. O. Bjorn, and M. M. Caldwell (1998), Changes in biologically active ultraviolet radiation reaching the Earth's surface, *J. Photochem. Photobiol. B*, *46*, 5–19.

McClellan, J., J. Sisco, B. Suarez, and G. Keogh (2010), Geoengineering cost analysis, *AR10-182*, 86 pp., Aurora Flight Sci., Cambridge, Mass.

Medalia, A. I., D. Rivin, and D. R. Sanders (1983), A comparison of carbon black with soot, *Sci. Total Environ.*, *31*(1), 1–22, doi:10.1016/0048-9697(83)90053-0.

Mills, M. J., O. B. Toon, R. P. Turco, D. E. Kinnison, and R. R. Garcia (2008), Massive global ozone loss predicted following regional nuclear conflict, *Proc. Natl. Acad. Sci. U. S. A.*, *105*(14), 5307–5312, doi:10.1073/pnas.0710058105.

Molina, M. J., L. T. Molina, T. B. Fitzpatrick, and P. T. Nghiem (2000), Ozone depletion and human health effects, in *Environmental Medicine*, edited by L. Moóller, pp. 28–51, Joint Ind. Safety Counc., Stockholm.

Nienow, A. M., and J. T. Roberts (2006), Heterogeneous chemistry of carbon aerosols, *Annu. Rev. Phys. Chem.*, *57*, 105–128, doi:10.1146/annurev.physchem.57.032905.104525.

Pressman, J., and P. Warneck (1970), The stratosphere as a chemical sink for carbon monoxide, *J. Atmos. Sci.*, *27*(1), 155–163.

Pueschel, R. F., S. Verma, H. Rohatschek, G. V. Ferry, N. Boiadjieva, S. D. Howard, and A. W. Strawa (2000), Vertical transport of anthropogenic soot aerosol into the middle atmosphere, *J. Geophys. Res.*, *105*(D3), 3727–3736, doi:10.1029/1999JD900505.

Rasch, P. J., S. Tilmes, R. P. Turco, A. Robock, L. Oman, C.-C. Chen, G. L. Stenchikov, and R. R. Garcia (2008), An overview of geoengineering of climate using stratospheric sulfate aerosols, *Philos. Trans. R. Soc. A*, *366*, 4007–4037, doi:10.1098/rsta.2008.0131.

Rayner, N. A., D. E. Parker, E. B. Horton, C. K. Folland, L. V. Alexander, D. P. Rowell, E. C. Kent, and A. Kaplan (2003), Global analyses of sea surface temperature, sea ice, and night marine air temperature since the late nineteenth century, *J. Geophys. Res.*, *108*(D14), 4407, doi:10.1029/2002JD002670.

Ricke, K. L., M. G. Morgan, and M. R. Allen (2010), Regional climate response to solar-radiation management, *Nat. Geosci.*, *3*, 537–541, doi:/10.1038/ngeo915.

Robock, A. (1988), Enhancement of surface cooling due to forest fire smoke, *Science*, *242*(4880), 911–913, doi:10.1126/science.242.4880.911.

Robock, A. (1991), Surface cooling due to forest fire smoke, *J. Geophys. Res.*, *96*(D11), 20,869–20,878, doi:10.1029/91JD02043.

Robock, A. (2000), Volcanic eruptions and climate, *Rev. Geophys.*, *38*, 191–219, doi:10.1029/1998RG000054.

Robock, A., L. Oman, G. L. Stenchikov, O. B. Toon, C. Bardeen, and R. P. Turco (2007a), Climatic consequences of regional nuclear conflicts, *Atmos. Chem. Phys.*, *7*, 2003–2012, doi:10.5194/acp-7-2003-2007.

Robock, A., L. Oman, and G. L. Stenchikov (2007b), Nuclear winter revisited with a modern climate model and current nuclear arsenals: Still catastrophci consequences, *J. Geophys. Res.*, *112*, D13107, doi:10.1029/2006JD008235.

Robock, A., L. Oman, and G. L. Stenchikov (2008), Regional climate responses to geoengineering with tropical and Arctic SO_2 injections, *J. Geophys. Res.*, *113*, D16101, doi:10.1029/2008JD010050.

Robock, A., A. Marquardt, B. Kravitz, and G. Stenchikov (2009), Benefits, risks, and costs of stratospheric geoengineering, *Geophys. Res. Lett.*, *36*, L19703, doi:10.1029/2009GL039209.

Rohatschek, H. (1996), Levitation of stratospheric and mesospheric aerosols by gravitophoresis, *J. Aerosol Sci.*, *27*(3), 467–475, doi:10.1016/0021-8502(95)00556-0.

Rose, D., B. Wehner, M. Ketzel, C. Engler, J. Voigtländer, T. Tuch, and A. Wiedensohler (2006), Atmospheric number size distributions of soot particles and estimation of emission factors, *Atmos. Chem. Phys.*, *6*, 1021–1031, doi:10.5194/acp-6-1021-2006.

Ross, M., M. Mills, and D. Toohey (2010), Potential climate impact of black carbon emitted by rockets, *Geophys. Res. Lett.*, *37*, L24810, doi:10.1029/2010GL044548.

Sato, M., et al. (2003), Global atmospheric black carbon inferred from AERONET, *Proc. Natl. Acad. Sci. U. S. A.*, *100*, 6319–6324.

Schmidt, G. A., et al. (2006), Present-day atmospheric simulations using GISS ModelE: Comparison to in situ, satellite and reanalysis data, *J. Clim.*, *19*, 153–192, doi:10.1175/JCLI3612.1.

Shindell, D. T., G. A. Schmidt, R. L. Miller, and D. Rind (2001), Northern Hemisphere winter climate response to greenhouse gas, ozone, solar, and volcanic forcing, *J. Geophys. Res.*, *106*(D7), 7193–7210, doi:10.1029/2000JD900547.

Shindell, D. T., G. Faluvegi, N. Unger, E. Aguilar, G. A. Schmidt, D. M. Koch, S. E. Bauer, and R. L. Miller (2006), Simulations of preindustrial, present-day, and 2100 conditions in the NASA GISS composition and climate model G-PUCCINI, *Atmos. Chem. Phys.*, *6*, 4427–4459, doi:10.5194/acp-6-4427-2006.

Solomon, S. (1999), Stratospheric ozone depletion: A review of concepts and history, *Rev. Geophys.*, *37*(3), 275–316, doi:10.1029/1999RG900008.

Solomon, S., M. Mills, L. E. Heidt, W. H. Pollock, and A. F. Tuck (1992), On the evaluation of ozone depletion potentials, *J. Geophys. Res.*, *97*(D1), 825–842, doi:10.1029/91JD02613.

Solomon, S., J. S. Daniel, R. R. Neely III, J. P. Vernier, E. G. Dutton, and L. W. Thomason (2011), The persistently variable "background" stratospheric aerosol layer and global climate change, *Science*, *333*(6044), 866–870, doi:10.1126/science.1206027.

SPARC CCMVal (2010), SPARC report on the evaluation of chemistry-climate models, edited by V. Eyring, T. G. Shepherd, and D. W. Waugh, *SPARC Rep. 5*, 426 pp., Univ. of Toronto, Toronto, Ont., Canada. [Available at http://www.sparc-climate.org/publications/sparc-reports/sparc-report-no5/.]

Stenchikov, G. L., I. Kirchner, A. Robock, H.-F. Graf, J. C. Antuña, R. G. Grainger, A. Lambert, and L. Thomason (1998), Radiative forcing from the 1991 Mount Pinatubo volcanic eruption, *J. Geophys. Res.*, *103*, 13,837–13,857, doi:10.1029/98JD00693.

Stern, N. (2006), *The Economics of Climate Change: The Stern Review, Executive Summary*, 27 pp., Her Majesty's Treasury, London. [Available at http://www.hm-treasury.gov.uk/d/Executive_Summary.pdf.]

Stevenson, D. S., R. M. Doherty, M. G. Sanderson, W. J. Collins, C. E. Johnson, and R. G. Derwent (2004), Radiative forcing from aircraft NO_x emissions: Mechanisms and seasonal dependence, *J. Geophys. Res.*, *109*, D17307, doi:10.1029/2004JD004759.

Stolarski, R. S., et al. (1995), 1995 scientific assessment of the atmospheric effects of stratospheric aircraft, *NASA Ref. Publ.*, *1381*, 105 pp.

Tang, I. N. (1996), Chemical and size effects of hygroscopic aerosols on light scattering coefficients, *J. Geophys. Res.*, *101*(D14), 19,245–19,250.

Teller, E., L. Wood, and R. Hyde (1997), Global warming and ice ages: I. Prospects for physics-based modulation of global change, *UCRL-JC-128715*, 18 pp., Lawrence Livermore Natl. Lab., Livermore, Calif.

Teller, E., R. Hyde, and L. Wood (2002), Active climate stabilization: Practical physics-based approaches to prevention of climate change, report, 8 pp., Lawrence Livermore Natl. Lab., Livermore, Calif.

Tilmes, S., R. Müller, and R. Salawitch (2008), The sensitivity of polar ozone depletion to proposed geoengineering schemes, *Science*, *320*, 1201–1204, doi:10.1126/science.1153966.

Tilmes, S., R. R. Garcia, D. E. Kinnison, A. Gettelman, and P. J. Rasch (2009), Impact of geoengineered aerosols on the troposphere and stratosphere, *J. Geophys. Res.*, *114*, D12305, doi:10.1029/2008JD011420.

Toon, O. B., A. Robock, R. P. Turco, C. Bardeen, L. Oman, and G. L. Stenchikov (2007), Consequences of regional-scale nuclear conflicts, *Science*, *315*, 1224–1225, doi:10.1126/science.1137747.

Turco, R. P., O. B. Toon, T. P. Ackerman, J. B. Pollack, and C. Sagan (1983), Nuclear winter: Global consequences of multiple nuclear explosions, *Science*, *222*(4630), 1283–1292, doi:10.1126/science.222.4630.1283.

T. W. Brown Oil Co., Inc. (1999), Material safety data sheet for #2 diesel, report, 2 pp., Ventura, Calif. [Available at http://www.mjmmasonry.com/safety/dieselfuelmsds.pdf.]

U.S. Energy Information Administration (EIA) (2010a), Global oil consumption, report, 2 pp., Washington, D. C. [Available at http://www.eia.doe.gov/pub/oil_gas/petroleum/analysis_publications/oil_market_basics/demand_text.htm.]

U.S. Energy Information Administration (EIA) (2010b), U.S. refining capacity, report, 2 pp., Washington, D. C. [Available at http://www.eia.doe.gov/pub/oil_gas/petroleum/analysis_publications/oil_market_basics/refining_text.htm#U.S. Refining Capacity.]

U.S. Environmental Protection Agency (EPA) (1995), Carbon black, in *AP 42 Compilation of Air Pollutant Emission Factors*, vol. I, 5th ed., pp. 6.1-1–6.1-10, U.S. Environ. Prot. Agency, Washington, D. C. [Available at http://www.epa.gov/ttnchie1/ap42/ch06/final/c06s01.pdf.]

U.S. Environmental Protection Agency (EPA) (1996), Gasoline and diesel industrial engines, in *AP 42 Compilation of Air Pollutant Emission Factors*, vol. I, 5th ed. update, pp. 3.3-1–3.3-9, U.S. Environ. Prot. Agency, Washington, D. C. [Available at http://www.epa.gov/ttnchie1/ap42/ch03/final/c03s03.pdf.]

U.S. Environmental Protection Agency (EPA) (2005), Average carbon dioxide emissions resulting from gasoline and diesel fuel, *EPA 420-F-05-001*, 3 pp., U.S. Environ. Prot. Agency, Washington, D. C. [Available online at http://www.epa.gov/oms/climate/420f05001.pdf.]

U.S. Environmental Protection Agency (EPA) (2009), Heavy-duty highway diesel program, report, Washington, D. C. [Available online at http://www.epa.gov/otaq/highway-diesel/index.htm.]

Van Haver, P., D. De Muer, M. Beekmann, and C. Mancier (1996), Climatology of tropopause folds at midlatitudes, *Geophys. Res. Lett.*, *23*(9), 1033–1036, doi:10.1029/96GL00956.

Vogelmann, A. M., A. Robock, and R. G. Ellingson (1988), Effects of dirty snow in nuclear winter simulations, *J. Geophys. Res.*, *93*(D5), 5319–5332, doi:10.1029/JD093iD05p05319.

Watson, A. Y., and P. A. Valberg (2001), Carbon black and soot: Two different substances, *AIHA J.*, *62*(2), 218–228, doi:10.1080/15298660108984625.

Weinstock, B., and H. Niki (1972), Carbon monoxide balance in nature, *Science*, *176*(4032), 290–292, doi:10.1126/science.176.4032.290.

Zhisheng, A., J. E. Kutzbach, W. L. Prell, and S. C. Porter (2001), Evolution of Asian monsoons and phased uplift of the Himalaya-Tibetan plateau since Late Miocene times, *Nature*, *411*, 62–66, doi:10.1038/35075035.